HHS Public Access

Author manuscript

Chem Rev. Author manuscript; available in PMC 2018 June 14.

Published in final edited form as:

Chem Rev. 2017 June 14; 117(11): 7457–7477. doi:10.1021/acs.chemrev.6b00716.

Super-resolution microscopy: shedding light on the cellular plasma membrane

Matthew B Stone[1], **Sarah A Shelby**[1], and **Sarah L Veatch**[1,*]

[1]Biophysics, University of Michigan, Chemistry 930 N University Ave, Ann Arbor 48109

Abstract

Lipids and the membranes they form are fundamental building blocks of cellular life, and their geometry and chemical properties distinguish membranes from other cellular environments. Collective processes occurring within membranes strongly impact cellular behavior and biochemistry, and understanding these processes presents unique challenges due to the often complex and myriad interactions between membrane components. Super-resolution microscopy offers a significant gain in resolution over traditional optical microscopy, enabling the localization of individual molecules even in densely labeled samples and in cellular and tissue environments. These microscopy techniques have been used to examine the organization and dynamics of plasma membrane components, providing insight into the fundamental interactions that determine membrane functions. Here, we broadly introduce the structure and organization of the mammalian plasma membrane and review recent applications of super-resolution microscopy to the study of membranes. We then highlight some inherent challenges faced when using super-resolution microscopy to study membranes, and we discuss recent technical advancements that promise further improvements to super-resolution microscopy and its application to the plasma membrane.

Graphical abstract

*Corresponding author, sveatch@umich.edu.

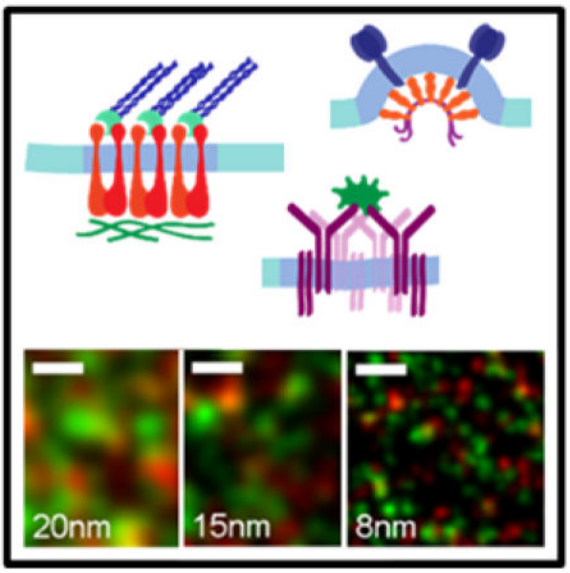

1 Introduction

The cell membrane is a complex mixture of lipids and proteins in close contact with the cortical cytoskeleton and the extracellular matrix, whose composition and dynamics is highly regulated through a vast array of cellular processes. In addition to its function as an electrical and physical barrier, the plasma membrane is the site of diverse cellular biochemistry responsible for regulating how the cell interacts with and responds to its environment. Signals that originate at the plasma membrane play a critical role in cell growth, differentiation, secretion, autocrine and paracrine signaling, and immunity, for example. While many of the protein players in these vital pathways have been identified, a more complete picture will illustrate how these molecules interact in time and space, and will describe the ways in which the complex landscape of the membrane modulates these interactions. Recent advances in fluorescence microscopy, single molecule and super-resolution imaging have contributed new information to these vital questions, and hold enormous promise for elucidating many features of the plasma membrane.

In the following pages, we provide an overview of the organizing principles that underlie plasma membrane structure and function, review how super-resolution microscopy approaches have shed light on processes occurring within membranes, and discuss some limitations faced by these methods when applied to studies of plasma membrane processes. Single molecule and super-resolution fluorescence microscopy has a long history within the study of membranes, where some of the earliest single molecule studies pioneered the observation of the motion and nanoscale organization of plasma membrane proteins. We briefly discuss this history and provide an extensive review of more recent work that characterizes plasma membrane structure and function through fluorescence-based super-resolution imaging methods. The plasma membrane imposes some specific challenges for experiments, and thus we discuss several technical considerations that are particularly applicable to super-resolution imaging of membranes, emphasizing the challenges in

observing clustering and co-localization of membrane components. Within this context, we present simple simulations illustrating the challenges and caveats of super-resolution localization microscopy with emphasis on quantitative data analysis using correlation functions. Recent advances in fluorescent probes, imaging technology, and data quantification have pushed the limits of super-resolution microscopy, and we conclude with our view on how these and other developments will shape future studies.

1.1 Anatomy of the mammalian plasma membrane

In their simplest form, bilayer membranes are composed of lipids surrounded by an aqueous fluid. Lipids are amphiphilic molecules with a hydrophilic headgroup and typically two hydrophobic hydrocarbon chains that collectively self-assemble into bilayer structures when placed in excess water. Lipid chains themselves are short polymers that can take on many confirmations within the hydrophobic core of the bilayer, helping to maintain the membrane as a two-dimensional fluid. Lipid headgroups are anchored at the oil-water interface, shielding the membrane core from the surrounding water and ions, and actin as the molecular interface with the surrounding fluids. Lipids in bilayers can be in a variety of physical states, with characteristic levels of mobility and molecular ordering. Bilayers can be in a rigid solid-like state often referred to as the gel phase, or in one of two more fluid liquid phases, or can contain mixtures of these phases[1–5]. The two liquid phases, called liquid-ordered and liquid-disordered are distinguished by their composition and physical properties such as membrane thickness and the extension of lipid hydrocarbon chains. Lipids can also assemble into non-bilayer topologies, including the highly curved inverse-hexagonal phase and cubic phases important for both biological processes and crystalizing membrane proteins[6–12]. These natural tendencies of lipids and lipid mixtures to self-organize in different ways provides the cell with a flexible toolbox, with the ability to tune membrane spontaneous curvature and stiffness, viscosity, ion permeability, and to even organize components within the membrane plane.

There is large chemical diversity of lipids in cellular membranes. This diversity is most easily seen in the lipid headgroups, which can vary in size, charge, and surface chemistry. There are two dominate types of linkages connecting headgroups to hydrophobic acyl chains, and the chains themselves can vary dramatically in length (number of carbons) and level of unsaturation. These chemical variations are combinatorically varied by enzymes involved in lipid metabolism, and as a result there are at least 800 distinct lipid species in a typical mammalian plasma membrane[13]. Cholesterol is by far the most abundant single lipid in the plasma membrane of mammalian cells, sometimes exceeding 40 mol% of total lipid[14,15]. The chemical structure of cholesterol is distinct from other cellular lipids: it is more hydrophobic, contains fused planar rings and a single short hydrocarbon chain[15]. Lipids can also be covalently modified with sugars or proteins, or can bind with high affinity to soluble proteins. This broad chemical diversity is highly regulated by cells in order to tune a broad array of physical and biological properties that are vital to its function. The molecular composition of lipids varies dramatically within cellular organelles and even within leaflets of the same bilayer, due to both lipid trafficking and biogenesis[2]. Recent efforts to quantitatively map lipid components using mass spectrometry have highlighted the vast diversity and interconnectivity of lipids[13,16,17]. In addition to acting as ligands and

signaling molecules, the molecular composition of lipids establishes collective physical properties of the membrane as a whole – properties such as electrical resistance, viscosity, bending rigidity, and electrostatic charge[18].

The plasma membrane also contains nearly 50% mass fraction of proteins[19]. These take the form of proteins that span the plasma membrane through a single alpha helical segment, proteins that traverse the membrane multiple times, and those that associate only with a single membrane leaflet[20] as illustrated graphically in Figure 1A. Many plasma membrane proteins are post-translationally modified with lipid chains, and some of these can be dynamically added and removed by enzymes resident within the plasma membrane itself [21]. The membrane association of soluble and peripheral proteins can be achieved through directly binding to lipids or membrane-embedded proteins, and is often regulated through enzymatic modification (e.g. phosphorylation) of both lipid and protein species[22–24]. Some proteins can bend or even break membranes, playing important roles in endocytosis and exocytosis, as well as viral fusion[25,26]. As with plasma membrane lipids, the protein content of the PM is highly regulated and dynamic. Both plasma membrane lipid and protein components can vary dramatically between cell types and during different stages of cellular development[27].

The plasma membrane is in direct physical contact with both the extracellular matrix and cortical cytoskeleton, depicted in Figure 1A. This association acts to add mechanical strength to the cellular interface, provides a means to control cell shape and mobility, and can dictate interactions with other cells or extracellular factors[28]. Association with these elements also influences the localization and dynamics of some membrane constituents. Many lipids and proteins facing the extracellular space are modified with sugars that directly intercalate into the extracellular matrix. The plasma membrane is also conjugated to the rigid protein filaments that make up the cortical cytoskeleton. This occurs through direct protein-protein and protein-lipid binding as well as through indirect coupling through electrostatics or fluid dynamics[29–32]. Inversely, membrane proteins and dynamics can influence the polymerization and reorganization of cytoskeletal networks, through the binding of actin-modifying proteins to phosphoinositides, for example membrane-bound WASP[33]. Taken together, the plasma membrane is a complex molecular assembly which is directly coupled to both the extracellular and intracellular spaces.

Membrane phases are also thought to influence the spatial organization of membrane components, and are conceptually shown in Figure 1A. Bilayer membranes made of purified lipids can undergo phase transitions between more ordered and more disordered fluid states, where more ordered phases have acyl chains that are more aligned resulting in tighter packing and a slightly thicker bilayer. These liquid-ordered and liquid-disordered phases can coexist in the same phase-separated membrane, similar to oil and water de-mixing in three dimensions. It is proposed that similar forces influence the lateral organization of intact plasma membranes[34], and in support of this cellular plasma membranes exhibit phase separation when isolated and examined at low temperature[35]. The concept that lipids can help organize proteins within cellular membranes is commonly referred to as the lipid raft hypothesis[36], and remains controversial in part due to the lack of reliable experimental methods to probe these membrane structures[37,38]. However, biophysical investigations have

provided support that the membrane can exhibit domains of relatively ordered or disordered membrane, especially around clustered proteins and receptors[39]. It is also thought that the tendency for plasma membrane lipids to assemble into non-lamellar phases can play important roles in functional processes that require membrane bending[8]. Understanding the impact of phase effects in the plasma membrane is an important goal for membrane research, as these subtle effects may influence a variety of processes occurring at the plasma membrane.

Membrane properties influence the nature of interactions between proteins that reside within the bilayer. Just like soluble proteins, membrane proteins can form complexes through electrostatic and Van der Waals interactions. Membranes tend to orient embedded protein binding sites, often lowering the entropic free energy cost to binding. These direct associations are responsible for the stability of many multi-protein complexes present among plasma membrane proteins. In membranes, proteins can also interact indirectly via interactions mediated through the membrane itself, as shown in Figure1A. These interactions tend to be weaker than those accessible through direct binding, but can act over larger distances. Examples include protein associations due to a shared preference for a specific membrane curvature, bilayer thickness, or membrane composition. Plasma membrane proteins and lipids are also often organized via interactions outside of the membrane plane. These can include interactions mediated through adhesion to another membrane surface[40], to protein assemblies proximal to the membrane[41], or through direct interactions with cytoskeletal or extracellular matrix components[42,43]. In a living membrane, biochemistry occurs within this complex and dynamic environment to provide a wide array of cellular functions.

Interactions between membrane components such as those detailed above can be cooperative and complex, and relevant biological events often exhibit a mixture of these interactions as shown in Figure 1B. Experimental investigation of membrane physical chemistry has thus been greatly aided by techniques that provide specific molecular information in the context of the intact membrane. Further, experimental methods that are compatible with cellular plasma membranes are of very high value due to the practically impossible task of reproducing the complex membrane environment *in vitro*. Among these methods, single molecule and super-resolution microscopy stands out due to their ability to observe the localization and dynamics of individual molecules and thus interpret the molecular interactions that are acting upon the molecule of interest.

1.2 Early single molecule and super-resolution investigations of the plasma membrane

Cell plasma membranes are particularly well-suited for single molecule and super-resolution studies. The plasma membrane is inherently two dimensional (2D), and it is often possible to orient the sample such that the 2D motion occurs entirely within a single focal plane of an optical microscope. Also, many membrane-bound lipids and proteins can be visualized through binding to modified ligands or antibodies that are simply incubated with live cells. Finally, the membrane has higher viscosity than the surrounding cytoplasm or extracellular space, slowing the motions of its membrane-bound constituents. These features enabled numerous early studies of the organization and mobility of membrane components.

In the first single particle tracking (SPT) studies in live cells, Barak and Webb reported on the motion of low density lipoprotein (LDL) receptors when bound to LDL particles pre-loaded with a lipophilic fluorescent dye[44,45]. Soon after, several groups established methods to visualize the motion of gold beads bound to membrane components with nanometer-scale accuracy[46–48]. The robust scattering of gold particles could be imaged using standard or differential interference contrast (DIC) microscopy over extended time-periods since gold particles do not exhibit photobleaching, allowing the tracking of particles at fast frame rates and for arbitrarily long times. Early experiments with gold probes were highly non-specific, such as colloidal gold conjugated to poly-L-lysine[49] or ConA[50]. Greater specificity for target labeling was achieved by coating beads with specific ligands, such as transferrin and α2-macroglobulin receptor[51], as well as EGF and E-cadherin[52].

Over the years, improvements in labeling, imaging, and camera technologies have made it such that most single molecule and SPT measurements are accomplished through fluorescence detection. The now common use of expressible fluorescent protein conjugates allow for specific and non-perturbative labeling of membrane proteins, and further developments in single molecule methods allowed the localization and tracking of proteins of interest labeled with GFP[53–56]. The development and commercialization of total internal reflection (TIR) microscopy has played an important role in this revolution[57,58], making it possible to confine illumination of fluorophores to within roughly 100nm of a glass surface. This allows for selective illumination of the plasma membrane of adherent cells while reducing background fluorescence, improving the detection of single fluorophores. Finally, driven largely by applications in astronomy, cameras have become more sensitive and efficient, and are now commonly able to detect single photons with increasingly fast acquisition rates. With modern cameras and imaging platforms, it has become routine to image and track the single molecule mobility of membrane proteins in a wide range of contexts. These studies have uncovered heterogeneity of motion within and between membrane components, and highlight the complexity of the plasma membrane environment[59,60].

Plasma membrane-associated proteins and lipids were among the initial targets for fluorescence-based super-resolution imaging methodologies since they allowed investigators to observe both the spatial distribution and dynamics of membrane components. The clustered spatial distributions of the viral membrane proteins Gag[61] and hemagglutinin[62] were observed with (fluorescence) photoactivation light microscopy ((f)PALM), and the 2D[63] and 3D[64] supramolecular structure of clathrin-coated vesicles was measured using stochastic optical reconstruction microscopy (STORM). The high resolution geometries of model membranes were also shown by Point Accumulation for Imaging in Nanoscale Topology (PAINT) with membrane partitioning fluorophores[65]. Dynamic maps of membrane component location and diffusion could now be produced from super-resolution point localization data, as was shown for the viral proteins VSVG and Gag [66] and adhesion complexes [67]. Further, stimulated emission depletion (STED) microscopy can create diffraction-unlimited excitation volumes, allowing for STED-fluorescence correlation spectroscopy (FCS) measurements of membrane component diffusion to elucidate nanometer scale trapping and non-linear diffusion of individual membrane components in live cells[68]. Since then, super-resolution fluorescence microscopy methods have been

broadly applied to the study of plasma and other membranes, resolving the spatial distribution and dynamics of important membrane components.

2 Super-resolution investigations of biological membranes

The plasma membrane has proved to be a useful system to demonstrate the power of single molecule and super-resolution approaches in cells. These methods have been applied to the study of numerous biological processes at the cell surface. Many structures present within the plasma membrane have characteristic length scales between 10 and 100 nm. This dimension is larger than the individual proteins and lipids that make up the membrane but smaller than the diffraction limit. Super-resolution microscopy enables the direct imaging of these structures, enabling their investigation in the context of intact, and often living cells. In this section, we review a subset of more recent work where super-resolution fluorescence microscopy techniques have been applied to better understand membrane receptors, membrane curvature, and lipid-mediated heterogeneity within membranes.

2.1 Membrane receptors

Membrane receptors allow the cell to sense its environment by translating varied extracellular stimuli into intracellular chemical signals. Drug therapies often target membrane receptors due to their accessibility on the external surface of the cell and because of the impact of signaling cascades on many facets of cellular behavior. Receptor signaling is carefully controlled by regulatory factors that can have diverse mechanisms, including direct interaction with specific signaling partners, assembly of signaling complexes around receptors, and receptor internalization. The local physical environment of the plasma membrane around receptors can influence these biochemical processes through both the distinct partitioning and activity of proteins within these environments. Fluorescence microscopy of receptors in their native membrane environment plays an important role in elucidating the function and interactions between receptors and regulatory proteins, and super-resolution microscopy gives high resolution information on receptor dynamics and spatial organization. Here we focus on recent applications of super-resolution microscopy to two broad classes of plasma membrane receptors, G protein coupled receptors (GPCRs) and immunoreceptors.

2.1.1 GPCRs—GPCRs are an important class of receptors as they mediate a wide variety of signaling outcomes and are also a widely-used target for drug therapies. GPCR conformational states determine the nature of interactions with heterotrimeric G proteins as well as signaling regulators such as arrestins[69–72]. There is growing evidence that the proper functioning of many GPCRs is dependent on their local membrane environment. This can take the form of modulation of receptor interactions with allosteric regulators, G proteins, or even local lipids. There is also active debate regarding the oligomeric state of many GPCRs and how this influences their function. These topics are being actively investigated using single-molecule and super-resolution approaches, and various labeling methods for GPCRs have been extensively reviewed[73] and include incorporation of unnatural amino acids into proteins, fluorescent labeling of GPCR ligands, and the use of nanobodies for labeling GPCRs.

β_2AR is a GPCR expressed in many cell types that mediates a diverse set of functions including blood vessel dilation, smooth muscle relaxation, and insulin secretion. Dimerization, oligomerization, and higher-order clustering has been implicated in the functional regulation of β_2AR function[74,75]. Early super-resolution studies using near field scanning optical microscopy (NSOM) reported self-clustering of β_2AR and association of clustered receptors with caveolae[76]. B_2AR was an early target for experiments aimed at molecular counting by PALM[77], and appears highly self-clustered in cardiomyocytes but not in other cell types where PALM microscopy was used to reconstruct super-resolved images of receptor positions[78]. The dynamics of β_2AR have also been studied extensively using single particle tracking methods, which find evidence for oligomerization[79,80] as well as a mechanistic role for the cytoskeleton in clustering and confinement of receptor motion[81].

Another commonly studied GPCR is the chemokine receptor CCR5, which is expressed on T-cells and also functions as a co-receptor for HIV. The spatial organization of the GPCR CCR5 was observed using D_2O-enhanced dSTORM microscopy, where D_2O was used to increase the fluorescence quantum yield and thus the precision of single particle localizations[82]. Other studies have probed CCR5-dependent changes in regulators of CCR5 signaling such as beta arrestin, which is involved in the removal of CCR5 from the plasma membrane[83,84], and have provided evidence that GPCR internalization is correlated with arrestin clustering independent of GPCR signaling. Super-resolution techniques have been used to investigate the spatial distribution of other GPCRs, such as CB1[85], which was shown to have a uniform spatial distribution within presynaptic boutons of various types, and luteinizing hormone receptor[86], for which functionally relevant mutations were suggested to exhibit distinct oligomerization patterns.

2.1.2 Immune receptors—Immune receptors recognize a wide array of antigens and are vital to the specific recognition and clearance of microbiological invasion. Since immune receptors function to direct inflammatory responses, they also play a role in many auto-immune diseases. Innate immune receptors such as the NOD and Toll-like receptors recognize specific antigens, whereas adaptive immune receptors undergo genetic adaptation and selection, which allow for the recognition of new antigens and pathogens. Cellular context and mesoscale organization of immune receptors are thought to influence their function, and this feature is reflected in the formation of the T cell- B cell immune synapse where multiple signaling molecules including the receptor are organized in a concentric manner[87,88]. Super-resolution imaging is an appropriate tool for studying the spatial organization in this system and thus it has been applied to many different immunoreceptor signaling systems.

T cell receptors (TCR) recognize antigen fragments bound within MHC proteins. Signaling through the TCR is regulated by a diverse array of adaptor and signaling proteins, and clustering of the receptor is thought to impact its function. The spatial organization of TCR and its signaling partner Linker for Activation of T cells (LAT)[89], the adaptor protein SLP-76, and the kinase ZAP-70[90], were examined using PALM. These experiments suggest that TCR and LAT exist in a self-clustered state prior to TCR activation and provide evidence that the spatial distributions of LAT, SLP-76, and ZAP-70 respond to TCR ligation[89,90]. The phosphorylation state of the receptor and associated signaling molecules

have also been investigated using super-resolution localization microscopy[91,92], and the correlation of cluster size and density with colocalization with phosphorylation suggests spatial distribution of TCR impacts its signaling[91]. Recent technical advances combining light sheet illumination and dSTORM imaging have also enabled high resolution imaging of the TCR within lymph nodes, and this study also suggests that TCR exists in a self-clustered distribution prior to binding antigen[93].

B cells are another crucial player in the adaptive immune system. The B cell receptor (BCR) recognizes intact antigen in the blood and lymph, and the successful maturation of B cells leads to the production of antibodies from former BCRs. Clustering of the BCR is known to be important for its function, as well as the interaction between BCR, the cytoskeleton, and adaptor proteins[94]. The spatial distribution of IgM, IgD, and IgG BCRs prior to and after receptor clustering by antigen has been investigated by several groups with dSTORM[95–97]. These studies suggest that BCR is self-clustered prior to binding antigen, and that clustering behavior is distinct for IgM vs IgD and IgM vs IgG BCRs. Additionally, the diffusion of BCR and CD19 were measured in wild type and CD81 knockout cells[96], suggesting that the diffusion of these proteins is influenced by an actin and tetraspannin network. BCR clustering and diffusion was also shown to be dependent on Ezrin expression in primary B cells[98], supporting the hypothesis that the actin network influences BCR organization and dynamics. The spatial colocalization and dynamics of BCR and Lyn in live cells was investigated with two color simultaneous STORM and PALM[99], which measured direct binding of Lyn to BCR through the reduction of Lyn mobility and colocalization with BCR following antigen stimulation.

Another well studied immune receptor is FcεRI, expressed primarily in mast cells and basophils, which binds 1:1 to soluble IgE antibodies and becomes activated upon receptor clustering. The organization and dynamics of FcεRI have been targets of single molecule and super-resolution investigation for decades[100–103]. One application of STORM simultaneously probed the mobility and localization of receptors in live cells undergoing signaling[104], and showed that slowdown and clustering of receptors in response to antigen begins prior to calcium release in these cells. FcεRI mobility and dynamics have also been studied utilizing FcεRI labeled with Fluorogen-activating proteins (FAPs)[103]. Similar to PAINT microscopy[65], FAP labels “blink” through transient binding of a cognate fluorogenic dye[105]. Single molecule tracking showed that the dynamics of the signal-transducing γ subunit of FcεRI is controlled by the IgE-binding α subunit. Additionally, a recent multi-color study in chemically fixed cells probed interactions between FcεRI and the kinase Lyn, showing that drug-induced perturbation of actin networks leads to increased interaction between receptors and Lyn[106].

Innate immune receptors have also been the target of super-resolution microscopy investigations. For example, the interaction between the immune receptor NOD1, its kinase RIP2, and bacterial peptidoglycan in early endosomes was observed using STORM microscopy[107]. Further, the clustering and co-clustering of the C-type lectins CD-SIGN and CD206, which mediate the uptake of pathogens, was investigated with Blink microscopy[108].

2.1.3 Other receptors—Many receptors have also been studied using super-resolution techniques. Glycine receptor is a ligand gated ion channel important for neuronal polarization, and splice variant α3L comprising of a 15 AA intracellular insert alters the receptor's gating and desensitization. It was shown that this longer splice variant exhibits a highly clustered membrane distribution in contrast to the shorter variant α3R[109]. Epidermal growth factor receptor (EGFR) mediates many aspects of cell growth and proliferation, and its function has been linked to its oligomerization and dimerization. EGFR dimerization was studied using a PAINT approach where fluorescently labeled EGF binding and unbinding served as the PAINT probe[110]. Further, EGFR clustering has been shown to be distinct between apical and basal membrane surfaces, suggesting that these two membrane environments play distinct roles in EGFR clustering[111]. Finally, natural killer T cells are crucially dependent upon their namesake receptor in order to deliver cytolytic granules to target cells. The spatial distribution of the cortical actin meshwork around Natural Killer TCR clusters was observed using 3D structured illumination microscopy (SIM)[112,113], which showed that the membrane-proximal actin meshwork is actively re-modeled in these cells to allow secretion of lytic granules.

2.1.4 General notes on the use of super-resolution microscopy to query receptor self-clustering—As evidenced by the wealth of research reviewed above, receptor clustering and spatial organization is a focal point for investigations into the signaling and regulation of many types of membrane receptors. Self-clustering of receptors, co-clustering of receptors with effector proteins and signaling partners, and other modes of spatial patterning can create specialized microenvironments where specific biochemical processes can be favored or suppressed. Although super-resolution fluorescence microscopy has been extensively used to query the clustering of receptors and effector proteins, distinct challenges prevent the simple interpretation of this data because it is difficult to simply distinguish monomers from small self-clustered oligomers by this method. This is a topic discussed more extensively in Sections 3.1 and 3.2 below.

2.2 Membrane organizational modes

Membranes are often organized over distances much longer than the sizes of individual molecules through cooperative interactions between membrane components. For example, membranes curve through the actions of numerous proteins and lipids[114], and the collective tendency for membrane components to phase separate leads to heterogeneity on the 10–100nm length-scale in both model membranes and cells[115]. Interactions between the plasma membrane, cortical cytoskeleton, and extracellular matrix are thought to be important in regulating the structures arising from collective interactions within the membrane plane, including the maintenance of overall cell shape and plasticity. Super-resolution fluorescence microscopy techniques are well suited for probing membrane organization on intermediate length-scales, and hold promise for revealing how individual molecules and their interactions shape the large-scale processes and collective behavior of the membrane.

2.2.1 Curvature—Curvature plays a role in a diverse set of processes occurring at the plasma membrane and within membrane-bound organelles. One important question is how this curvature arises and how proteins and lipids react to and maintain membrane curvature.

Super-resolution allows the location of individual proteins to be resolved with respect to the local membrane curvature, and can illuminate membrane curvature in areas that are difficult to reach with traditional microscopy.

Individual proteins are generally much smaller than the length scale of relevant membrane curvature, yet it has been suggested that they can both sense and localize to sites of curvature, and can also stabilize the formation of large membrane deformations when working in tandem [114]. This distinction between curvature sensing and active membrane remodeling was explored using 3D SIM in the context of the behavior of the septin CDC11. Here, SIM allowed for collection of high resolution images of membrane topology and protein spatial distribution, enabling geometric classification of membrane regions and colocalization analysis [116]. CDC11 proteins were found to localize to areas of high positive curvature, and polymerization of CDC11 stabilzes its association with the membrane. Similarly, SIM imaging of the negative curvature-preferring ESCRT complex found that ESCRT proteins preferentially localized to high negative curvature regions of a supported bilayer system, and assembled a ring of enrichment where negative curvature was the highest[117]. These experiments illustrate that highly curved membrane structures involve a combination of complex nucleation through sensing of existing curvature and co-operative assembly of curvature-favoring proteins. Caveolae are poorly characterized invaginated membrane structures that exhibit high curvature[118]. The caveolin Cav-1 was imaged in the context of living zebrafish embryos[119] and with respect to cytokine receptor[120] using PALM microscopy, which showed that assembly of caveolae was important for initiation of receptor signaling. Curvature is also involved in the assembly of structures on the membrane, such as in viral budding and virion formation, which requires deformation of the membrane. The immune system has adapted mechanisms to sense this deformation through expression of the protein tetherin, and super-resolution localization techniques have been used to clarify the role of curvature in its mechanism of action to inhibit formation of the virion[121].

Super-resolution microscopy can also shed light on membrane deformation events and large scale membrane shape changes that occur in the context of the plasma membrane and internal organelles through labeling of the lipid bilayer itself. The size distribution of mitochondria and ER organelles, the diffusion of individual dye molecules within these structures, and the fusion and fission between the mitochondrial and ER membranes was queried with STORM using lipophilic membrane dyes [122]. The restricted orientation of lipophilic dyes in the lipid bilayer can also be used to examine the orientation and topology of the membrane using fluorescent molecule localization under polarized light[123]. This scheme is an extension of pTIRFM, which is able to differentiate between membrane orientations by selecting dye molecules based on their alignment with a polarized TIRF excitation field[124].

2.2.2 Phase-like membrane heterogeneity—It has been hypothesized that heterogeneous distributions of membrane components can arise within plasma membranes as a consequence of favorable interactions between particular classes of lipids. Originally referred to as ‘lipid rafts’ [36], these membrane heterogeneities are now understood to be highly transient and very small (10–100nm), making them difficult to study by conventional fluorescence means[39]. Super-resolution microscopy has been applied to observe the spatial

distribution as well as dynamics of membrane components that are hypothesized to be heterogeneously sorted into membrane domains.

Numerous measurements have explored raft heterogeneity by monitoring the self-clustering of membrane associated proteins, for example[125–128]. Another more robust method to monitor partitioning into ordered domains is to localize a protein of interest alongside a marker known to partition with ordered lipids. Two common markers are GPI-linked proteins and cholera toxin B subunit (CTxB)[129]. Multicolor STORM and PALM have shown non-random spatial correlation between clustered GPI and actin[130], CTxB and EGFR[111], as well as between GPI and the μ-opioid receptor[131], suggesting that these proteins have favorable interactions with order-preferring lipids. We have also showed the exclusion of a disordered favoring probe from BCR clusters in live cells, supporting the hypothesis that ordered domains exist around BCR clusters[99]. Additionally, ordered membrane domains are thought to have slightly increased hydrophobic thickness, and dual-color STED microscopy was used to show the co-clustering of SNARE proteins as a function of their transmembrane domain length[132].

The diffusion of membrane components is thought to be different in the ordered and disordered domains, and thus trapping and anomalous diffusion have also been used as proxies for membrane domains[128,133–135]. However, recent work has shown that viscosity and compositional differences between the two domains may be small compared to what is observed in purified membranes, and diffusion is more strongly influenced by the cytoskeleton and other factors [43]. This may explain why one recent study did not detect evidence for “rafts” when monitoring the mobility or distribution of probes in a plasma membrane adhered to a patterned support [136]. STED-FCS can measure molecular diffusion within small areas of the plasma membrane spanning only a few tens of nanometers. This technique revealed that the sphingomyelin lipids, but not other lipid types, are transiently immobilized in the plasma membrane [43,137]. This pinning is cytoskeleton-dependent, and suggests a general mechanism through which cytoskeleton pinning sites may template ordered and disordered domains in the plasma membrane[138]. In reconstituted systems, similar coupling between membrane and cytoskeletal elements acts to modulate membrane domains when imaged using STED microscopy[139].

Separate from ordered and disordered domain demixing, it has been suggested that electrostatic interactions between certain acidic phospholipids can meditate their clustering and domain formation[140]. Super-resolution STED microscopy was used to observe the clustering of $PI(4,5)P_2$ in PC12 membrane sheets[141]. This study also provides evidence that $PI(4,5)P_2$ acts to regulate the clustering of proteins containing polybasic domains, such as those containing polybasic sequences. The clustering of these proteins being mediated by $PI(4,5)P_2$ is also supported by work in model membranes[141,142]. The spatial distribution of $PI(4,5)P_2$ and $PI(3,4,5)P_3$ was also examined using STORM microscopy, where authors have reported contrasting results of both a clustered[143] and uniform[144] distribution of these lipids in the plasma membrane. Future work will be necessary to reveal the true spatial distribution of this biochemically important class of lipids.

2.2.3 The cortical cytoskeletal and its regulation of membrane structure—The integrity of cell morphology depends on the anchorage of the plasma membrane to the cytoskeletal architecture. Complex co-ordination of both the cytoskeleton and membrane are required for large-scale changes in cell morphology such as those that occur during cell migration and cytokinesis. Furthermore, certain cell types may contain complex structures incorporating the cytoskeleton and the membrane in order to perform specialized tasks. Interactions between the membrane lipids and the cytoskeleton can have varying degrees of specificity; certain lipids can interact strongly with immobilized cytoskeletal elements through specific binding sites, and some proteins bind to the plasma membrane by less specific mechanisms such as charge and hydrophobic embedding. Super-resolution microscopy techniques reveal the detailed ultrastructure of the membrane and cytoskeleton and indicate the nature of the interactions.

Specialized cellular structures often require complex coordination between the cytoskeleton and membrane. Dual objective STORM was employed to observe the 3D ultrastructure of the cortical actin cytoskeleton, revealing distinctions between the dorsal and ventral layers [145]. Sensitive STED-FCS experiments have been be used to infer the size of the actin meshwork and show that cortical actin restricts phospholipid diffusion in a manner that depends upon the actin remodeling protein Arp2/3 [146]. Liver sinusoidal endothelial cells exhibit a pore-like structure which allows the filtration of objects between the blot and hepatocytes based on size selection. The spatial distribution of the cytoskeleton and plasma membrane was observed in liver sinusoidal endothelial cells using combination 3D-SIM and STORM microscopy, revealing a close association between the membrane and cytoskeleton [147]. A periodic structure of actin, spectrin, ankyrin and sodium channels was shown in neuronal axons using STORM microscopy, revealing a strikingly regular assembly of these cytoskeletal elements[148]. This periodic actin structure was also observed in both the axons and dendrites of living neurons using STED[149]. Axons also are often wrapped by myelin, multiple membranes that form a sheath around axons, helping to protect axons and assisting in nerve pulse propagation. STED-FCS also showed that lipid diffusion was faster and less confined in myelin, possibly due to the lack of cytoskeletal networks in these structures [150]. Further, the mobility of the viral protein hemagglutinin (HA) is restricted by membrane-proximal actin, and the spatial organization of actin-binding proteins around HA clusters suggests a dynamic co-regulation of the cytoskeleton and viral proteins[151].

Large scale shape changes within the cytoskeletal and membrane network are vital for the growth and maturation of cells and tissues and play important roles in cancer metastasis as well as normal cellular development. Cytoskeletal fibers conduct contractility forces along the cell, however, determining the forces acting on specific fiber classes has proven difficult. 3D SIM was employed to observe the spatial patterning of stress fibers during motility and large scale shape changes, allowing for the forces acting on specific cytoskeletal elements to be mapped[152]. Related to this, the molecular spatial composition of cell adhesions were also mapped using iPALM[153]. Further, new applications of STED to traction force microscopy allow for increased resolution for measuring the forces that cells exert on extracellular substrates [154].

3 Promise and challenges of super-resolution imaging applied to complex biological membranes

As a two-dimensional fluid comprised of a complex mixture of lipids and proteins, the plasma membrane provides a unique environment which cells utilize to accomplish a broad array of functions, a few of which are described above. This environment also presents unique challenges to experimental investigations. In the sections below, we describe several features of membranes and super-resolution imaging methods that present specific experimental obstacles, with a focus on fluorescence localization based super-resolution techniques. We also suggest how advances in super-resolution fluorescence microscopy may provide new approaches to overcome these obstacles.

3.1 Obstacles to molecular counting in super-resolved images

A common theme in membrane biology is that nano-sized assemblies of membrane components are often required to accomplish some cellular function[155]. These assemblies can be protein homo- or hetero dimers, small oligomers, or complexes where direct binding occurs between proteins and lipids, and these complexes can additionally be highly dynamic. The detailed stoichiometry of these complexes can impact the functional regulation of the proteins involved, and characterizing the stoichiometry of these assemblies is often considered important for understanding their molecular mechanisms.

Several robust fluorescence-based methods exist for counting molecules within protein complexes when complexes are well separated on the cell surface[156]. These include inferring the copy number of proteins present by calibrating the molecular brightness of single fluorophores and the variance of the fluorescence signal. Another routinely used method is to observe the sequential step-wise photobleaching of labeled proteins within complexes. In this method, one counts the molecular constituents by counting quantized decreases in brightness with the help of filtering algorithms and statistical methods. Both methods require that fluorophores are conjugated to target proteins at a 1:1 ratio, which is often accomplished by expressing the protein conjugated to a single fluorescent protein. Both of these methods have been applied successfully in a range of contexts [157–160], but require that individual oligomers are separated by distances much greater than the diffraction limit of visible light. Super-resolution methods such as stimulated emission or STED microscopy reduce this resolution limit and therefore enable this type of quantitative imaging on more densely labeled samples.

Molecular counting in super-resolution fluorescence localization microscopy measurements has proven to be more challenging[161]. This is because most fluorophores used for localization microscopy either blink reversibly, or are capable of activating multiple times before being bleached into an irreversible dark state. This effect is compounded if target molecules are labeled with proteins or antibodies that can be conjugated with multiple fluorophores, or if antibodies can bind to multiple sites on single target proteins. We refer to this effect as over-counting, since a single labeled molecule is observed several times in the same position. Fluorophores can also under-count the components they label. This can occur when activation occurs stochastically and data are not acquired for a long enough time to

fully sample all fluorophores. There are well documented situations where fluorophores are systematically under-counted. For example, there is often a finite population of photo-activatable or photo-switchable fluorophores that do not activate or switch into an observable state[162–166], and reductive caging of organic fluorophores often leads to some probes losing their ability to activate[167]. Also, some fluorophores quench when in close proximity to protein residues or other fluorophores[168–170]. These issues with over and under- counting are not limited to investigations of membrane proteins, but have been studied mostly in this context. Some examples of mechanisms that can give rise to over- and under-counting are shown in Figure 2A.

Several methods have been developed to compensate for the systematic over- and under-counting of single probes when a large number of target proteins are imaged. One method is to simply calibrate the average number of times a given probe is observed in a sparsely labeled sample imaged under the same conditions[130,171]. When probes are sparsely distributed, it is often assumed that all times a fluorophore is localized in the same position, it occurs due to multiple observations of the same target protein. This experiment can be used to calibrate the average number of probes localized within regions of interest in a more densely labeled sample as long as antibodies can only bind target proteins at single sites. Regions within a super-resolved image can be segmented using clustering algorithms such as DBSCAN[172], ClusterViSu[173], or other home-built algorithms[174], which are used to define extended objects within point resolved images.

More statistically sophisticated methods to count the average number of probes present in a segmented region have been devised, however most require some calibration of probe photo-physics and reactivation statistics[175,176]. These methods report on the stoichiometry of the average cluster because each individual observation has an intrinsically high variance. In cases where probe blinking is irreversible, or is reversible only within a finite time-window, and proteins are labeled with single fluorophores, it is in principle possible to count the number of proteins in complexes, although currently this is only reported for a small subset of proteins and fluorophores[177,178]. A simulated example that graphically highlights some of the pitfalls facing molecular counting in super-resolution fluorescence localization data is shown in Figure 2B. When stoichiometry and over-counting are low, the relative variation on the number of events in a given complex is high, making estimation of true stoichiometry within individual complexes difficult.

3.2 Labels appear self-clustered when super-resolved images are under-sampled and over-counted

The properties of fluorophores and labeling strategies that result in over-counting artifacts are also part of what make them useful for localization microscopy – if for some reason a label is not localized in one image frame, there is a finite probability that a label originating from the same labeled molecule will be observed on a second (or third) occasion if the sample is imaged over time. Observing single labeled molecules multiple times also produces more visually pleasing reconstructed images (Figure 2B), and provides a means to estimate localization precision from a dataset without relying on the outputs of fitting algorithms[179,180]. As discussed above, a negative consequence of over-counting is that it is

difficult to distinguish single labeled molecules from small clusters of labeled molecules. While this has the obvious implications for molecular counting discussed above, it has analogous effects on measures of self-clustering that are less appreciated in the literature. Over-counting impacts measures of self-clustering even when each labeled molecule is observed only once on average. This is because the probability of observing the same molecule multiple times always increases (and often dominates) the probability of detecting several localizations in the same super-resolved position [179].

Another important aspect that determines the quality of super-resolved images is spatial sampling, or how well the labeled molecules sample the underlying structures present in the system. An example is shown graphically in Figure 3A. Most super-resolved images of membranes are under-sampled, in that labeled molecules are separated by distances that are much greater than the localization precision of the measurement. This will be discussed in the particular context of compositionally complex membranes in section 3.6 below. Figure 3B shows simulated super-resolved images of the same structure at both low and high spatial sampling. The most visually pleasing and statistically significant images are obtained under conditions of high spatial sampling and high over-counting. Most often, super-resolved images of membranes are made up of components that are over-counted and poorly sample space. These images resemble collections of self-clustered spots that often require careful statistical analysis in order to extract information regarding the lateral distributions of the objects that they are labeling.

There are several methods available to quantify average self-clustering and co-clustering from super-resolved images that do not rely on molecular counting. Pair correlation functions quantify the average local density as a function of distance around an average probe[130,179]. A related measure, the Ripley's K or H functions, quantify the local density within a given radius and reports its statistical significance away from a random distribution[127,181]. Both of these measures are impacted by over-counting when only a single color is imaged [179], although in some cases it is possible to estimate and correct for the contributions of over-counting. Figure 3B and C show how single color images and their quantifications are impacted by over-counting, with over-counting producing higher levels of aberrant self-clustering when images are poorly sampled in space. This effect can be thought of intuitively: at low spatial sampling, the image only contains information on the location and apparent size of a few labeled molecules, while at high spatial sampling, the underlying structure begins to emerge.

Conveniently, over-counting does not impact quantifications of colocalization when two distinguishable probes are imaged[179]. This is demonstrated in Figure 3E, where the cross-correlation between two distinguishable probes remains consistent for a wide range of sampling densities, beyond effects on signal-to-noise. Over-counting and under-sampling also impacts the sensitivity of quantitative super-resolution measurements, which is discussed in detail in subsequent sections and figures.

3.3 Labeling lipids and membranes often alters their function

Lipids are small biomolecules that contain both hydrophobic and hydrophilic regions and rely on subtle variation in chemical structure to convey different physical and biological

properties. Because of this, it is often not possible to label lipids with a fluorophore while retaining its full functional identity. Several considerations for labeling lipids applicable to conventional and super-resolution fluorescence imaging are discussed below.

It is possible to directly conjugate certain lipids to fluorophores via headgroup modifications (most commonly for the case of PE, but also for other lipids), or through fluorescent conjugation of fatty acid chains. In both cases, the addition of the fluorophore dramatically alters lipid structure, both in the addition of bulk and in the modification of chemical and physical properties. The molecular weight of a typical lipid is roughly 750 g/mol, which is not much larger than even small fluorophores such as fluorescein (323 g/mol) or rhodamine (479 g/mol). When using chain-modified lipids it is important to consider that fluorophore structures do not resemble the linear hydrocarbon acyl chains that they replace and will greatly impact physical properties. For the case of headgroup-modified lipids, the hydrophobic nature of many fluorophores can lead to surprising changes in lipid physical properties. For example, most headgroup-labeled lipid probes partition with more disordered lipids even when the unconjugated form is expected to prefer the ordered phase[35,182]. Similar results are found for unmodified vs. fluorescently modified cholesterol. One successful strategy to overcome this perturbation is to instead conjugate the fluorophore via an extended hydrophilic linker[182–184]. In this case the resulting probe does not closely resemble the specific molecular structure of the lipid being emulated, but it can capture components of its behavior.

Another common strategy is to fluorescently tag proteins that bind to specific lipid headgroups. Examples include bacterial or fungal toxins that can be labeled and added exogenously and that bind specifically to outer leaflet lipids such as gangliosides or cholesterol. Lipid-binding peptides or proteins conjugated to fluorescent proteins or tags can also be expressed in cells. Several considerations need to be made when using proteins to tag lipids. First, a protein-bound lipid has dramatically different structural and physical properties than a free lipid, so its localization or dynamics may not accurately represent that of the free lipid. For example, a $PI(4,5)P_2$ lipid usually caries a charge of −3[185], but this electrostatic charge is shielded by divalent cations[186], and may mediate $PI(4,5)P_2$ clustering and higher order interactions[187]. $PI(4,5)P_2$ binding domains compete for binding with divalent cations[188], and can thus alter the behavior of $PI(4,5)P_2$. Also, many toxins that bind gangliosides tend to bind multivalently, clustering their bound lipids. An example is cholera toxin B subunit (CTxB) which can bind to up to 5 GM1 lipids[189]. In model membranes, CTxB binding can induce the formation of ordered membrane domains[190,191], and there is evidence that simply labeling the plasma membrane with CTxB can invoke a cellular signaling response[192–194].

A separate concern is that labeling lipids through protein binding acts to prevent the specific lipid component from participating in its normal function. A good example of this phenomenon is cholesterol binding by the fungal toxin Filipin, which is used to both label and perturb cholesterol in cells[195]. Another example is phosphatidylinositol (PI) binding domains. PI lipids bound by the probe are no longer able to bind to other endogenous protein domains, resulting in altered rates of hydrolysis and possibly other biochemical functions[196]. One strategy to overcome potential complications evoked by lipid-binding proteins and

peptides is to probe membranes with proteins that bind with low affinity, although there is some evidence that lower affinity probes are more likely to oligomerize upon membrane binding, which is also perturbative[23]. This perturbation is worsened in the case of high over-expression, thus expressing proteins at endogenous levels using CRISPR/CAS9 genetic knock-in techniques is an attractive potential solution[197]. In all cases, care needs to be taken in the design and interpretation of experiments where lipids are labeled.

Of special relevance to super-resolution microscopy studies of membranes, many fluorescent proteins themselves tend to oligomerize, which can significantly change the behavior of labeled proteins. The photoactivatable protein mEos2 is a popular PALM probe due to its brightness, photostability, and compatibility with buffers needed for STORM and organic fluorophore photoswitching[198]. However, it has been shown to form homodimers[166,199]. This dimerization behavior can be accentuated in membranes, where binding sites are oriented and the probability of collisions between labeled proteins is often increased due to the reduced dimensionality of this system[200,201]. The photoactivatable proteins mEos3.2, Dronpa2, and mMaple3 were shown to be relatively free of this dimerization potential using a ClpP reporter clustering assay[166], however this does not rule out dimerization of these fluorescent proteins.

3.4 Membrane components are not easily chemically fixed

The vast majority of super-resolution imaging experiments are conducted on chemically fixed cells, since it often takes tens of seconds to tens of minutes to acquire a single reconstructed image. Most chemical fixation techniques work by using aldehydes to form chemical cross-links between reactive lysine groups abundant on proteins. Most lipids are not strongly reactive with aldehydes and therefore remain mobile even after chemical fixation. Exceptions to this are those lipids that contain amine groups (such as phosphoethanolamine and phosphoserine), and the production of unstable hemiacetals during reactions between alcohols and aldehydes. Membrane proteins and peptides also tend to be less accessible to chemical fixatives and require harsher fixation methods than are typically required for studies involving soluble proteins[202]. Another problem is fixation protocols that involve ‘cytosolic washout’ steps. These usually involve co-incubation of samples with a weak fixative and a detergent such as TritonX-100. TritonX-100 is well known to partition into membranes and selectively solubilize certain membrane components[203,204], therefore can dramatically alter membrane structure.

It remains an open question if chemical fixation produces structure within membranes. Fixation itself can induce large-scale vesiculation of the plasma membrane[205]. In our experience, we obtain good quantitative agreement in colocalization measurements conducted in live cells and in cells chemically fixed with paraformaldehyde and glutaraldehyde in the absence of calcium[99], suggesting that fixation does not impact membrane organization at least in this specific context. Another common sample preparation procedure is to produce membrane sheets by sheering adherent cells off a surface prior to chemical fixation[89,206]. Although this method can preserve many structural aspects membranes when done quickly[207], it is still not known how it impacts the subtle structure that super-resolution methods have the sensitivity to detect. Finally, incomplete fixation with

only paraformaldehyde and followed by primary antibody labeling can lead to spurious clustering of membrane proteins detected by super-resolution microscopy [208]. Importantly, addition of glutaraldehyde can prevent post-fixation antibody-induced clustering. Care should be taken when interpreting super-resolution microscopy data from chemically fixed cells, and when possible observed spatial distributions should be compared to measurements in live cells or between fixation conditions.

3.5 Super-resolution imaging of the dynamic membrane

Super-resolution microscopy in live cells offers a wealth of data on the dynamics of biological structures and as well as the components that comprise the structures, however temporal resolution limits and harsh experimental conditions need to be carefully considered when applying these techniques to live cells. Biological structures have a variety of characteristic lifetimes that can depend on cellular and environmental contexts. For example, even in the absence of cell motility and chemoattractant stimulation, cortical actin filaments in *Dictyostelium discoideum* undergo rearrangements on the scale of seconds or longer[209], whereas rapidly diffusing individual lipids diffuse at around 4μm^2/s and are only rarely immobilized in one location[137]. Super-resolution microscopy image reconstruction has an intrinsically limited temporal resolution, since subsets of molecules must be observed independently in STORM, PALM, and STED methodologies.

Advancements in STED microscopy allow for images to be reconstructed in 0.2s using a beam-scanning variant of STED[210], and advances to sCMOS camera technology and analysis algorithms have allowed for reconstruction of super-resolved images at high frame rates[211]. However, super-resolution microscopy can also lend important information that does not rely upon reconstructing images of particle locations. The single molecule dynamics and cross-correlation between two diffusing super-resolved objects can be obtained simultaneously using steady-state cross-correlation methodologies which compile correlation functions over a time window[99]. Additionally, the dynamics of individual molecules can be queried with extremely high temporal and spatial resolution using STED-FCS[137]. These correlation functions should be averaged over time windows ideally smaller than the timescales of any cellular process being investigated. The specialized buffers and high illumination powers required for some modes of super-resolution imaging can also stress live cells, leading to altered behaviors[212,213]. In cases where systems under investigation are not amenable to super-resolution imaging or single particle tracking, dynamics can also be queried using correlative variants of traditional microscopy, such as Bayesian Total Internal Reflection Fluorescence Correlation Spectroscopy (TIR-FCS)[214] and spatiotemporal image correlation spectroscopy (STICS)[215].

3.6 Membranes contain thousands of different molecular species

A major characteristic of the plasma membrane is its vast molecular diversity. There are nearly 800 distinct lipid species in a typical plasma membrane[13], and roughly half of the membrane by weight is made up of proteins[19]. This differs dramatically from other cellular structures frequently visualized by super-resolution microscopy such as microtubules and other cytoskeletal elements or clathrin-coated pits, where a single protein species or a small collection of proteins makes up the majority of a given structure. The consequence of this

molecular diversity is that imaging any one element will necessarily produce a picture of the plasma membrane that appears under-sampled as long as probes are immobile. For example, if an experiment is imaging an abundant membrane protein present at several hundred per square micron (for example an immune receptor that is highly expressed on an immune cell surface), then these proteins would be on average 10–50nm apart if they are all randomly distributed. A less abundant protein might be present at ten copies per square micron, and these would be separated by on average 300nm if randomly distributed. One consequence of this inherent under-sampling is that super-resolved images of membrane proteins often resemble a collection of spots rather than filled in structures, as illustrated in Figures 2 and 3. Another consequence of low molecular density is that image quantification methods aimed at examining colocalization will have reduced signal-to-noise when interactions are weak or occur on short length-scales.

3.7 Membranes are not always flat

One major advantage of studying the plasma membrane with light microscopy is that it tends to spread into a relatively flat sheet at the glass-water interface of a microscope cover-glass and can be forced to adhere to surfaces by coating them with adhesion molecules. This geometry is well suited to TIR microscopy, in which excitation light penetrates only a few hundred nanometers past the substrate. This approach provides a significant increase in signal-to-noise and enables quantitative localization and tracking of labeled membrane components.

Although the membrane of adherent cells tends to be flat, many topological features may still exist that complicate this interpretation, especially with the resolution and sensitivity provided by super-resolution imaging methods. For example, cellular structures such as podosomes[216], microvilli[217,218], and filopodia[219] can create significant topology that can lead to the false interpretation of organization within the membrane plane when only a 2D projection is imaged. Consideration of membrane topology may be particularly important in phagocytes and other cells which have natural ruffling and excess membrane to accommodate large scale membrane and cellular shape transitions and bending [218]. Three-dimensional STORM[64], PALM, iPALM [220], and STED [221] can be applied for this purpose, and sequential photobleaching using multi-angle TIRF imaging also yields axial resolution[222]. For example, STORM was utilized[64] to resolve the half-spherical structure of clathrin coated pits with a diameter of 180 nm. However, some topological features may not be resolvable by these techniques because the resolution achieved by STORM and PALM with commonly used fluorophores may be less than the radius of curvature of interest. Finally, it is important to note that membrane topology and curvature can affect the measurement of membrane protein diffusion, clustering, and co-clustering as reviewed elsewhere [223].

3.8 Weak interactions have low contrast

In addition to the strongly associated protein-protein and protein-lipid complexes described above, functional processes that occur in membranes also exploit weak associations, such as those driven by curvature, electrostatics, or compositional heterogeneity often referred to as “lipid rafts”. The interaction energies involved in these processes tend to be less than the

thermal energy (1 k_BT, where k_B is the Boltzman constant and T is temperature in units of Kelvin). This is much smaller than typical protein-protein interactions, such as the binding of SH2 domains to phosphorylated peptides, which vary from 6 to 15 k_BT[224], although some soluble proteins bind to lipids with energies approaching these values[225]. While membrane-mediated interactions may be weak, they can impact cellular biochemistry because individual molecules can act collectively to maintain robust structures. Nonetheless, membrane components that interact weakly will necessarily be less co-localized than those that interact strongly, and this presents some complications in the execution and interpretation of experimental results. This is highlighted in Figure 4, which shows that apparent co-clustering and calculated correlation functions depend on both density of colocalized structures (Figure 4A,B) and the strength of partitioning of each molecule into these structures (Figure 4C,D). Figure 4A,B demonstrates that co-clusters need to be sparsely distributed with respect to the localization precision in order to be detected. Figure 4C,D illustrates that colocalization within even sparse complexes can be difficult to detect when a large percentage of labeled molecules are present outside of complexes. Overall, colocalization is often hard to simply visualize in an image due effects such as spatial under-sampling, over-counting, weak interactions, and low molecular density. Consequently, measurements of colocalization generally require quantification methods that involve averaging over multiple areas or multiple cells to reach statistical significance.

When imaging with a single color, apparent self-clustering arising from over-counting of single target molecules often dominates measurements when probing weak signals like those described above. This is because it is often much more likely for a single fluorophore to blink multiple times within a 20nm radius than for there to be multiple molecules within that radius, especially if molecules are distributed uniformly. The exception would be if the molecules were present at very high local densities, such as occurs after a receptor has been cross-linked with a multivalent ligand or when membrane-associated proteins assemble into macromolecular structures such as a nascent viral bud or clathrin-coated pit. While there are methods to correct for counting effects, this component usually dominates self-clustering observations in a way that makes it difficult to accurately account for in post processing. A better strategy is to produce distinguishable molecules labeled with different colors. In this case, when two differently colored events are observed in the same location, there is no ambiguity with regards to whether the two signals originated from different labeled molecules vs. the same molecule.

Colocalization within multi-color images can suffer from systematic errors when there is spectral overlap between the probes used. For example, problems can arise when the emission of blue-shifted fluorophores bleeds into the emission channel for a second red-shifted probe. In extreme cases, bleed through can lead to misidentification of signals observed in the red-shifted channel. In less extreme cases, the presence of weak fluorescence emission intensity in the red-shifted channel can bias the localization of a true red-shifted probe detected simultaneously. This is of particular relevance for live cell imaging, when it is often most useful to probe localizations detected simultaneously or nearly simultaneously[99]. We have also encountered unexpected sources of cross-talk in point localized super-resolution imaging measurements, such as far red probes detected in our near-red emission channel due to imperfect filters, anti-Stokes shifts, and fluorescent

impurities[99,226]. In addition, commonly used BODIPY fluorophores can undergo photoconversion in the presence of high laser intensity, altering the chemical nature and photophysical behavior of the dye[227]. Overall, it is vital to control for all sources of cross-talk and to make estimates on how even minimal bleed-through levels impact experimental outcomes.

The cross-talk artifacts described above will tend to produce results indicating more co-localization than is present in actual molecular distributions. One way to gain confidence in a result of clustering or co-clustering is to include controls expected to produce less coclustering, random codistributions or exclusion while utilizing the same fluorescent probes. For example, the vast majority of existing data supporting the concept of lipid rafts only probes the self-clustering or co-clustering of membrane components. We have been able to recently show that disordered-favoring markers are weakly excluded from BCR clusters, and Lyn is less strongly recruited to BCR upon kinase inhibition treatment[99]. These observations generate additional confidence in the imaging and analysis methods used, and do not rely upon observations of cluster size or density.

3.9 Higher resolution gives better sensitivity

Localization-based super-resolution microscopy provides an order of magnitude increase in resolution compared to traditional microscopy. However, this method has not yet achieved resolution on the order of the size of individual proteins or molecules. Super-resolution particle localization methods such as STORM and PALM rely upon isolating individual fluorescent events and estimating the center of the fluorophore from the intensity distribution of this event. The precision of this localization scales by the inverse square of the number of photons recorded from the fluorescent event[218]. Thus, a four-fold increase in fluorophore brightness will yield a two-fold increase spatial resolution. Advances in the quantum efficiency of photon detection, increases in fluorescent molecule brightness and photostability, as well as improved control over the fraction of probes in dark states all result in better resolution. Other factors also contribute to reducing image resolution from this theoretical limit, and addressing these issues improves resolution. These factors include stage drift[229], fluorophore orientation effects[230], the finite size of labeling antibodies[231], and registration error between emission channels[232].

Just as in diffraction limited microscopy, better resolution does not simply improve the ability to observe small structures. Instead, it improves the ability to distinguish two structures situated in close proximity. This principal is illustrated in Figure 5A,B where co-clustering of two components in a crowded field of molecular complexes becomes easier to detect as resolution is improved. When structures are small, higher resolution also acts to improve image contrast, since signals detected from the small structure are spread out over a smaller area. This improves contrast because the total number of detected signals remains constant, as does the total area represented by the cross-correlation function. This principal is illustrated in Figure 5C,D where the partial co-clustering of two components in a sparse field of molecular complexes becomes easier to detect as resolution is improved.

4 Future outlook

Over the past decade, super-resolution imaging methods have enabled an important step forward in how researchers view and investigate biological membranes, providing relatively simple access to length-scales relevant to macromolecular biological assemblies within intact cells and tissues. This high resolution view of the cell membrane has led to both elucidation of existing questions in membrane research as well as the development of new questions regarding the molecular underpinnings of membrane structure and function. Advances in imaging hardware, fluorescent probes, and analyses algorithms push resolution limits to even smaller length scales.

Super-resolution microscopy has the potential to benefit many aspects of membrane biology and biophysics research, and the relative ease of these experimental systems allows simple implementation for researchers with a range of backgrounds. Super-resolution microscopes, including those for STED, STORM, PALM, and SIM have been commercialized, and can practically be used “off the shelf”. Faster and more robust image processing algorithms make these methods more computationally feasible than ever before, and broadly distributed image software exists for a wide range of experimental data. Further, solid-state lasers have become available in a wider range of wavelengths and with higher output power. These models are smaller, less expensive, and simpler to handle over time, allowing for even modest microscope setups to take advantage of some modern super-resolution techniques.

Major technological advances in recent years hold great promise for improving the resolution and sensitivity of point localization based super-resolution methods. For one, SCMOS based detection modalities allow for large fields of view to be imaged at fast acquisition rates, enabling video rate image reconstruction for live cell imaging[211]. Each year brings new improvements in this image acquisition technology, with recent commercially available detectors incorporating back-illuminated chips with quantum efficiency approaching 95% in the visible range. Recent years have also seen the development of new synthetic and protein based fluorescent probes. These probes have improved photo-physical properties, are more membrane permeable, and extend further over the spectral range, enabling the detection of more distinct labels with higher localization precision and at higher molecular densities[233,234]. Some synthetic probes are now available in a caged, non-fluorescent form[233,235] that can be selectively activated with a UV light-source. This feature provides another knob for the experimenter to turn to optimize imaging conditions for particular applications and allows better signal-to-noise of single molecule detection without the need for high readout illumination intensity. There have also been some notable improvements in the illumination of samples. For one, higher power continuous wave lasers are becoming more accessible, making it easier to control the blinking characteristics of existing synthetic fluorophores, improving their localization precision and enhancing the labeling densities accessible to experiments. Further, the use of ultrahigh numerical aperture and TIRF excitation has achieved large improvements in SIM resolution[236]. As shown in Figures 4 and 5, these resolution gains help to not only see smaller objects, but also to resolve interactions between weakly associating components in dense environments. Super-resolution modalities are being combined to yield novel methodologies, such as structured illumination microscopy with structured

photoactivation[236], light sheet microscopy with two photon excitation[237], and structured illumination microscopy with two photon excitation[238], allowing for improved spatial resolution and the ability to image deep into thick samples. Finally, there have been large improvements in the technology for localizing fluorophores in the third dimension. These include phase retrieval[239–241], point spread function engineering[242,243], and interferometric PALM microscopy[244], some of which are straight forward to implement on an existing super-resolution microscope.

Together, these technical improvements have the potential to push resolution and sensitivity to new levels, enabling scientists to ask and answer new questions. In the context of the plasma membrane, continuous improvements to these tools could enable the observation and quantification of molecular interactions between individual membrane components, even when these interactions are weak or collective. Improved resolution in three dimensions will allow for researchers to fully map out the macromolecular organization of signaling complexes or other membrane associated structures, allowing the identification of conserved higher order structures within molecular complexes. Utilizing these tools in live cells will allow for the study of functional processes in their native context. Current technology is already advancing how we think about the behavior of individual molecules in membranes even as we must think critically about limits of this technology, as well as the realities associated with molecular diversity, stochasticity, and the need to incorporate statistical models for understanding cellular processes. Finally, pushing these tools into live cells will allow for the study of processes in their native context at an unprecedented level of detail, allowing researchers to probe the physical mechanisms underlying biological functions. In the light of these technical advances, the underlying details of macromolecular membrane structure can begin to come into focus.

Acknowledgments

This work is supported by the National Institutes of Health (R01GM110052) and the National Science Foundation (MCB-1552439).

References

1. Veatch SL, Keller SL. Seeing Spots: Complex Phase Behavior in Simple Membranes. Biochim Biophys Acta BBA - Mol Cell Res. 2005; 1746(3):172–185.
2. van Meer G, Voelker DR, Feigenson GW. Membrane Lipids: Where They Are and How They Behave. Nat Rev Mol Cell Biol. 2008; 9(2):112–124. [PubMed: 18216768]
3. Lewis RNAH, McElhaney RN. Membrane Lipid Phase Transitions and Phase Organization Studied by Fourier Transform Infrared Spectroscopy. Biochim Biophys Acta BBA - Biomembr. 2013; 1828(10):2347–2358.
4. Elson EL, Fried E, Dolbow JE, Genin GM. Phase Separation in Biological Membranes: Integration of Theory and Experiment. Annu Rev Biophys. 2010; 39(1):207–226. [PubMed: 20192775]
5. Heberle FA, Feigenson GW. Phase Separation in Lipid Membranes. Cold Spring Harb Perspect Biol. 2011; 3(4)
6. Caffrey M. A Comprehensive Review of the Lipid Cubic Phase or in Meso Method for Crystallizing Membrane and Soluble Proteins and Complexes. Acta Crystallogr Sect F Struct Biol Commun. 2015; 71(Pt 1):3–18. [PubMed: 25615961]
7. Cullis PR, de Kruijff B. Lipid Polymorphism and the Functional Roles of Lipids in Biological Membranes. Biochim Biophys Acta. 1979; 559(4):399–420. [PubMed: 391283]

8. Frolov VA, Shnyrova AV, Zimmerberg J. Lipid Polymorphisms and Membrane Shape. Cold Spring Harb Perspect Biol. 2011; 3(11):a004747. [PubMed: 21646378]
9. Jouhet J. Importance of the Hexagonal Lipid Phase in Biological Membrane Organization. Front Plant Sci. 2013; 4
10. Gruner SM, Cullis PR, Hope MJ, Tilcock CPS. Lipid Polymorphism: The Molecular Basis of Nonbilayer Phases. Annu Rev Biophys Biophys Chem. 1985; 14(1):211–238. [PubMed: 3890880]
11. Seddon JM. Structure of the Inverted Hexagonal (HII) Phase, and Non-Lamellar Phase Transitions of Lipids. Biochim Biophys Acta. 1990; 1031(1):1–69. [PubMed: 2407291]
12. Tenchov B. On the Reversibility of the Phase Transitions in Lipid-Water Systems. Chem Phys Lipids. 1991; 57(2):165–177. [PubMed: 2054902]
13. Levental KR, Lorent JH, Lin X, Skinkle AD, Surma MA, Stockenbojer EA, Gorfe AA, Levental I. Polyunsaturated Lipids Regulate Membrane Domain Stability by Tuning Membrane Order. Biophys J. 2016; 110(8):1800–1810. [PubMed: 27119640]
14. Cooper RA. Influence of Increased Membrane Cholesterol on Membrane Fluidity and Cell Function in Human Red Blood Cells. J Supramol Struct. 1978; 8(4):413–430. [PubMed: 723275]
15. Yeagle PL. Cholesterol and the Cell Membrane. Biochim Biophys Acta BBA - Rev Biomembr. 1985; 822(3):267–287.
16. Köberlin MS, Snijder B, Heinz LX, Baumann CL, Fauster A, Vladimer GI, Gavin AC, Superti-Furga G. A Conserved Circular Network of Coregulated Lipids Modulates Innate Immune Responses. Cell. 2015; 162(1):170–183. [PubMed: 26095250]
17. Shevchenko A, Simons K. Lipidomics: Coming to Grips with Lipid Diversity. Nat Rev Mol Cell Biol. 2010; 11(8):593–598. [PubMed: 20606693]
18. Ernst R, Ejsing CS, Antonny B. Homeoviscous Adaptation and the Regulation of Membrane Lipids. J Mol Biol. 2016
19. Dodge JT, Mitchell C, Hanahan DJ. The Preparation and Chemical Characteristics of Hemoglobin-Free Ghosts of Human Erythrocytes. Arch Biochem Biophys. 1963; 100(1):119–130. [PubMed: 14028302]
20. Steck TL. The Organization of Proteins in the Human Red Blood Cell Membrane. A Review. J Cell Biol. 1974; 62(1):1–19. [PubMed: 4600883]
21. Resh MD. Trafficking and Signaling by Fatty-Acylated and Prenylated Proteins. Nat Chem Biol. 2006; 2(11):584–590. [PubMed: 17051234]
22. Cho W, Stahelin RV. Membrane-Protein Interactions in Cell Signaling and Membrane Trafficking. Annu Rev Biophys Biomol Struct. 2005; 34(1):119–151. [PubMed: 15869386]
23. Lemmon MA. Membrane Recognition by Phospholipid-Binding Domains. Nat Rev Mol Cell Biol. 2008; 9(2):99–111. [PubMed: 18216767]
24. Singer SJ. The Molecular Organization of Membranes. Annu Rev Biochem. 1974; 43(1):805–833. [PubMed: 4277710]
25. Südhof TC, Rothman JE. Membrane Fusion: Grappling with SNARE and SM Proteins. Science. 2009; 323(5913):474–477. [PubMed: 19164740]
26. White JM, Delos SE, Brecher M, Schornberg K. Structures and Mechanisms of Viral Membrane Fusion Proteins. Crit Rev Biochem Mol Biol. 2008; 43(3):189–219. [PubMed: 18568847]
27. Aviram R, Manella G, Kopelman N, Neufeld-Cohen A, Zwighaft Z, Elimelech M, Adamovich Y, Golik M, Wang C, Han X, et al. Lipidomics Analyses Reveal Temporal and Spatial Lipid Organization and Uncover Daily Oscillations in Intracellular Organelles. Mol Cell. 2016; 62(4): 636–648. [PubMed: 27161994]
28. Bezanilla M, Gladfelter AS, Kovar DR, Lee WL. Cytoskeletal Dynamics: A View from the Membrane. J Cell Biol. 2015; 209(3):329–337. [PubMed: 25963816]
29. Luna EJ, Hitt AL. Cytoskeleton--Plasma Membrane Interactions. Science. 1992; 258(5084):955–964. [PubMed: 1439807]
30. Sheetz MP. Cell Control by Membrane–cytoskeleton Adhesion. Nat Rev Mol Cell Biol. 2001; 2(5): 392–396. [PubMed: 11331914]

31. Sheetz MP, Sable JE, Döbereiner HG. Continuous Membrane-Cytoskeleton Adhesion Requires Continuous Accommodation to Lipid and Cytoskeleton Dynamics. Annu Rev Biophys Biomol Struct. 2006; 35(1):417–434. [PubMed: 16689643]
32. Tserkovnyak Y, Nelson DR. Conditions for Extreme Sensitivity of Protein Diffusion in Membranes to Cell Environments. Proc Natl Acad Sci U S A. 2006; 103(41):15002–15007. [PubMed: 17008402]
33. Saarikangas J, Zhao H, Lappalainen P. Regulation of the Actin Cytoskeleton-Plasma Membrane Interplay by Phosphoinositides. Physiol Rev. 2010; 90(1):259–289. [PubMed: 20086078]
34. Machta BB, Veatch SL, Sethna JP. Critical Casimir Forces in Cellular Membranes. Phys Rev Lett. 2012; 109(13):138101. [PubMed: 23030121]
35. Baumgart T, Hunt G, Farkas ER, Webb WW, Feigenson GW. Fluorescence Probe Partitioning between Lo/Ld Phases in Lipid Membranes. Biochim Biophys Acta. 2007; 1768(9):2182–2194. [PubMed: 17588529]
36. Simons K, Ikonen E. Functional Rafts in Cell Membranes. Nature. 1997; 387(6633):569–572. [PubMed: 9177342]
37. Kenworthy AK. Have We Become Overly Reliant on Lipid Rafts? Talking Point on the Involvement of Lipid Rafts in T-Cell Activation. EMBO Rep. 2008; 9(6):531–535. [PubMed: 18516088]
38. Munro S. Lipid Rafts: Elusive or Illusive? Cell. 2003; 115(4):377–388. [PubMed: 14622593]
39. Simons K, Gerl MJ. Revitalizing Membrane Rafts: New Tools and Insights. Nat Rev Mol Cell Biol. 2010; 11(10):688–699. [PubMed: 20861879]
40. Albersdörfer A, Feder T, Sackmann E. Adhesion-Induced Domain Formation by Interplay of Long-Range Repulsion and Short-Range Attraction Force: A Model Membrane Study. Biophys J. 1997; 73(1):245–257. [PubMed: 9199789]
41. Banjade S, Rosen MK. Phase Transitions of Multivalent Proteins Can Promote Clustering of Membrane Receptors. eLife. 2014; 3:e04123.
42. Chaudhuri A, Bhattacharya B, Gowrishankar K, Mayor S, Rao M. Spatiotemporal Regulation of Chemical Reactions by Active Cytoskeletal Remodeling. Proc Natl Acad Sci U S A. 2011; 108(36):14825–14830. [PubMed: 21873247]
43. Mueller V, Ringemann C, Honigmann A, Schwarzmann G, Medda R, Leutenegger M, Polyakova S, Belov VN, Hell SW, Eggeling C. STED Nanoscopy Reveals Molecular Details of Cholesterol- and Cytoskeleton-Modulated Lipid Interactions in Living Cells. Biophys J. 2011; 101(7):1651–1660. [PubMed: 21961591]
44. Barak LS, Webb WW. Fluorescent Low Density Lipoprotein for Observation of Dynamics of Individual Receptor Complexes on Cultured Human Fibroblasts. J Cell Biol. 1981; 90(3):595–604. [PubMed: 6270157]
45. Barak LS, Webb WW. Diffusion of Low Density Lipoprotein-Receptor Complex on Human Fibroblasts. J Cell Biol. 1982; 95(3):846–852. [PubMed: 6296157]
46. De Brabander M, Geuens G, Nuydens R, Moeremans M, De Mey J. Probing Microtubule-Dependent Intracellular Motility with Nanometre Particle Video Ultramicroscopy (Nanovid Ultramicroscopy). Cytobios. 1985; 43(174S):273–283. [PubMed: 3907999]
47. Gelles J, Schnapp BJ, Sheetz MP. Tracking Kinesin-Driven Movements with Nanometre-Scale Precision. Nature. 1988; 331(6155):450–453. [PubMed: 3123999]
48. Schnapp BJ, Gelles J, Sheetz MP. Nanometer-Scale Measurements Using Video Light Microscopy. Cell Motil Cytoskeleton. 1988; 10(1–2):47–53. [PubMed: 3141071]
49. de Brabander M, Nuydens R, Ishihara A, Holifield B, Jacobson K, Geerts H. Lateral Diffusion and Retrograde Movements of Individual Cell Surface Components on Single Motile Cells Observed with Nanovid Microscopy. J Cell Biol. 1991; 112(1):111–124. [PubMed: 1670778]
50. Sheets ED, Simson R, Jacobson K. New Insights into Membrane Dynamics from the Analysis of Cell Surface Interactions by Physical Methods. Curr Opin Cell Biol. 1995; 7(5):707–714. [PubMed: 8573346]
51. Sako Y, Kusumi A. Compartmentalized Structure of the Plasma Membrane for Receptor Movements as Revealed by a Nanometer-Level Motion Analysis. J Cell Biol. 1994; 125(6):1251–1264. [PubMed: 8207056]

52. Kusumi A, Sako Y, Yamamoto M. Confined Lateral Diffusion of Membrane Receptors as Studied by Single Particle Tracking (Nanovid Microscopy). Effects of Calcium-Induced Differentiation in Cultured Epithelial Cells. Biophys J. 1993; 65(5):2021–2040. [PubMed: 8298032]
53. Dickson RM, Cubitt AB, Tsien RY, Moerner WE. On/off Blinking and Switching Behaviour of Single Molecules of Green Fluorescent Protein. Nature. 1997; 388(6640):355–358. [PubMed: 9237752]
54. Heim R, Cubitt AB, Tsien RY. Improved Green Fluorescence. Nature. 1995; 373(6516):663–664.
55. Iwane AH, Funatsu T, Harada Y, Tokunaga M, Ohara O, Morimoto S, Yanagida T. Single Molecular Assay of Individual ATP Turnover by a Myosin-GFP Fusion Protein Expressed in Vitro. FEBS Lett. 1997; 407(2):235–238. [PubMed: 9166906]
56. Pierce DW, Hom-Booher N, Vale RD. Imaging Individual Green Fluorescent Proteins. Nature. 1997; 388(6640):338–338. [PubMed: 9237750]
57. Axelrod D. Cell-Substrate Contacts Illuminated by Total Internal Reflection Fluorescence. J Cell Biol. 1981; 89(1):141–145. [PubMed: 7014571]
58. Axelrod D, Burghardt TP, Thompson NL. Total Internal Reflection Fluorescence. Annu Rev Biophys Bioeng. 1984; 13:247–268. [PubMed: 6378070]
59. Kusumi A, Tsunoyama TA, Hirosawa KM, Kasai RS, Fujiwara TK. Tracking Single Molecules at Work in Living Cells. Nat Chem Biol. 2014; 10(7):524–532. [PubMed: 24937070]
60. Saxton MJ, Jacobson K. Single-Particle Tracking: Applications to Membrane Dynamics. Annu Rev Biophys Biomol Struct. 1997; 26:373–399. [PubMed: 9241424]
61. Betzig E, Patterson GH, Sougrat R, Lindwasser OW, Olenych S, Bonifacino JS, Davidson MW, Lippincott-Schwartz J, Hess HF. Imaging Intracellular Fluorescent Proteins at Nanometer Resolution. Science. 2006; 313(5793):1642–1645. [PubMed: 16902090]
62. Hess ST, Gould TJ, Gudheti MV, Maas SA, Mills KD, Zimmerberg J. Dynamic Clustered Distribution of Hemagglutinin Resolved at 40 Nm in Living Cell Membranes Discriminates between Raft Theories. Proc Natl Acad Sci U S A. 2007; 104(44):17370–17375. [PubMed: 17959773]
63. Bates WM, Huang B, Dempsey GT, Zhuang X. Multicolor Super-Resolution Imaging with Photo-Switchable Fluorescent Probes. Science. 2007; 317(5845):1749–1753. [PubMed: 17702910]
64. Huang B, Wang W, Bates M, Zhuang X. Three-Dimensional Super-Resolution Imaging by Stochastic Optical Reconstruction Microscopy. Science. 2008; 319(5864):810–813. [PubMed: 18174397]
65. Sharonov A, Hochstrasser RM. Wide-Field Subdiffraction Imaging by Accumulated Binding of Diffusing Probes. Proc Natl Acad Sci U S A. 2006; 103(50):18911–18916. [PubMed: 17142314]
66. Manley S, Gillette JM, Patterson GH, Shroff H, Hess HF, Betzig E, Lippincott-Schwartz J. High-Density Mapping of Single-Molecule Trajectories with Photoactivated Localization Microscopy. Nat Methods. 2008; 5(2):155–157. [PubMed: 18193054]
67. Shroff H, Galbraith CG, Galbraith JA, Betzig E. Live-Cell Photoactivated Localization Microscopy of Nanoscale Adhesion Dynamics. Nat Methods. 2008; 5(5):417–423. [PubMed: 18408726]
68. Eggeling C, Ringemann C, Medda R, Schwarzmann G, Sandhoff K, Polyakova S, Belov VN, Hein B, von Middendorff C, Schönle A, et al. Direct Observation of the Nanoscale Dynamics of Membrane Lipids in a Living Cell. Nature. 2009; 457(7233):1159–1162. [PubMed: 19098897]
69. Lefkowitz RJ, Shenoy SK. Transduction of Receptor Signals by β-Arrestins. Science. 2005; 308(5721):512–517. [PubMed: 15845844]
70. Kobilka BK, Deupi X. Conformational Complexity of G-Protein-Coupled Receptors. Trends Pharmacol Sci. 2007; 28(8):397–406. [PubMed: 17629961]
71. Sounier R, Mas C, Steyaert J, Laeremans T, Manglik A, Huang W, Kobilka BK, Déméné H, Granier S. Propagation of Conformational Changes during μ-Opioid Receptor Activation. Nature. 2015; 524(7565):375–378. [PubMed: 26245377]
72. Rosenbaum DM, Rasmussen SGF, Kobilka BK. The Structure and Function of G-Protein-Coupled Receptors. Nature. 2009; 459(7245):356–363. [PubMed: 19458711]
73. Tian H, Fürstenberg A, Huber T. Labeling and Single-Molecule Methods To Monitor G Protein-Coupled Receptor Dynamics. Chem Rev. 2016

74. Bouvier M. Oligomerization of G-Protein-Coupled Transmitter Receptors. Nat Rev Neurosci. 2001; 2(4):274–286. [PubMed: 11283750]
75. Szidonya L, Cserző M, Hunyady L. Dimerization and Oligomerization of G-Protein-Coupled Receptors: Debated Structures with Established and Emerging Functions. J Endocrinol. 2008; 196(3):435–453. [PubMed: 18310440]
76. Ianoul A, Grant DD, Rouleau Y, Bani-Yaghoub M, Johnston LJ, Pezacki JP. Imaging Nanometer Domains of Beta-Adrenergic Receptor Complexes on the Surface of Cardiac Myocytes. Nat Chem Biol. 2005; 1(4):196–202. [PubMed: 16408035]
77. Annibale P, Vanni S, Scarselli M, Rothlisberger U, Radenovic A. Quantitative Photo Activated Localization Microscopy: Unraveling the Effects of Photoblinking. PLoS ONE. 2011; 6(7):e22678. [PubMed: 21818365]
78. Scarselli M, Annibale P, Radenovic A. Cell Type-Specific β2-Adrenergic Receptor Clusters Identified Using Photoactivated Localization Microscopy Are Not Lipid Raft Related, but Depend on Actin Cytoskeleton Integrity. J Biol Chem. 2012; 287(20):16768–16780. [PubMed: 22442147]
79. Calebiro D, Rieken F, Wagner J, Sungkaworn T, Zabel U, Borzi A, Cocucci E, Zürn A, Lohse MJ. Single-Molecule Analysis of Fluorescently Labeled G-Protein–coupled Receptors Reveals Complexes with Distinct Dynamics and Organization. Proc Natl Acad Sci. 2013; 110(2):743–748. [PubMed: 23267088]
80. Kasai RS, Kusumi A. Single-Molecule Imaging Revealed Dynamic GPCR Dimerization. Curr Opin Cell Biol. 2014; 27:78–86. [PubMed: 24480089]
81. Valentine CD, Haggie PM. Confinement of β(1)- and β(2)-Adrenergic Receptors in the Plasma Membrane of Cardiomyocyte-like H9c2 Cells Is Mediated by Selective Interactions with PDZ Domain and A-Kinase Anchoring Proteins but Not Caveolae. Mol Biol Cell. 2011; 22(16):2970–2982. [PubMed: 21680711]
82. Lee SF, Vérolet Q, Fürstenberg A. Improved Super-Resolution Microscopy with Oxazine Fluorophores in Heavy Water. Angew Chem Int Ed. 2013; 52(34):8948–8951.
83. Díez LT, Bönsch C, Malkusch S, Truan Z, Munteanu M, Heilemann M, Hartley O, Endesfelder U, Fürstenberg A. Coordinate-Based Co-Localization-Mediated Analysis of Arrestin Clustering upon Stimulation of the C–C Chemokine Receptor 5 with RANTES/CCL5 Analogues. Histochem Cell Biol. 2014; 142(1):69–77. [PubMed: 24623038]
84. Truan Z, Tarancón Díez L, Bönsch C, Malkusch S, Endesfelder U, Munteanu M, Hartley O, Heilemann M, Fürstenberg A. Quantitative Morphological Analysis of arrestin2 Clustering upon G Protein-Coupled Receptor Stimulation by Super-Resolution Microscopy. J Struct Biol. 2013; 184(2):329–334. [PubMed: 24091038]
85. Dudok B, Barna L, Ledri M, Szabó SI, Szabadits E, Pintér B, Woodhams SG, Henstridge CM, Balla GY, Nyilas R, et al. Cell-Specific STORM Super-Resolution Imaging Reveals Nanoscale Organization of Cannabinoid Signaling. Nat Neurosci. 2015; 18(1):75–86. [PubMed: 25485758]
86. Jonas KC, Fanelli F, Huhtaniemi IT, Hanyaloglu AC. Single Molecule Analysis of Functionally Asymmetric G Protein-Coupled Receptor (GPCR) Oligomers Reveals Diverse Spatial and Structural Assemblies. J Biol Chem. 2015; 290(7):3875–3892. [PubMed: 25516594]
87. Huppa JB, Davis MM. T-Cell-Antigen Recognition and the Immunological Synapse. Nat Rev Immunol. 2003; 3(12):973–983. [PubMed: 14647479]
88. Yuseff MI, Pierobon P, Reversat A, Lennon-Duménil AM. How B Cells Capture, Process and Present Antigens: A Crucial Role for Cell Polarity. Nat Rev Immunol. 2013; 13(7):475–486. [PubMed: 23797063]
89. Lillemeier BF, Mörtelmaier MA, Forstner MB, Huppa JB, Groves JT, Davis MM. TCR and Lat Are Expressed on Separate Protein Islands on T Cell Membranes and Concatenate during Activation. Nat Immunol. 2010; 11(1):90–96. [PubMed: 20010844]
90. Sherman E, Barr V, Manley S, Patterson G, Balagopalan L, Akpan I, Regan CK, Merrill RK, Sommers CL, Lippincott-Schwartz J, et al. Functional Nanoscale Organization of Signaling Molecules Downstream of the T Cell Antigen Receptor. Immunity. 2011; 35(5):705–720. [PubMed: 22055681]

91. Pageon SV, Tabarin T, Yamamoto Y, Ma Y, Bridgeman JS, Cohnen A, Benzing C, Gao Y, Crowther MD, Tungatt K, et al. Functional Role of T-Cell Receptor Nanoclusters in Signal Initiation and Antigen Discrimination. Proc Natl Acad Sci. 2016; 113(37):E5454–E5463. [PubMed: 27573839]

92. Williamson DJ, Owen DM, Rossy J, Magenau A, Wehrmann M, Gooding JJ, Gaus K. Pre-Existing Clusters of the Adaptor Lat Do Not Participate in Early T Cell Signaling Events. Nat Immunol. 2011; 12(7):655–662. [PubMed: 21642986]

93. Hu YS, Cang H, Lillemeier BF. Superresolution Imaging Reveals Nanometer- and Micrometer-Scale Spatial Distributions of T-Cell Receptors in Lymph Nodes. Proc Natl Acad Sci. 2016; 113(26):7201–7206. [PubMed: 27303041]

94. Mattila PK, Batista FD, Treanor B. Dynamics of the Actin Cytoskeleton Mediates Receptor Cross Talk: An Emerging Concept in Tuning Receptor Signaling. J Cell Biol. 2016; 212(3):267–280. [PubMed: 26833785]

95. Maity PC, Blount A, Jumaa H, Ronneberger O, Lillemeier BF, Reth M. B Cell Antigen Receptors of the IgM and IgD Classes Are Clustered in Different Protein Islands That Are Altered during B Cell Activation. Sci Signal. 2015; 8(394):ra93–ra93. [PubMed: 26373673]

96. Mattila PK, Feest C, Depoil D, Treanor B, Montaner B, Otipoby KL, Carter R, Justement LB, Bruckbauer A, Batista FD. The Actin and Tetraspanin Networks Organize Receptor Nanoclusters to Regulate B Cell Receptor-Mediated Signaling. Immunity. 2013; 38(3):461–474. [PubMed: 23499492]

97. Lee J, Sengupta P, Brzostowski J, Lippincott-Schwartz J, Pierce SK. The Nanoscale Spatial Organization of B Cell Receptors on IgM- and IgG-Expressing Human B Cells. Mol Biol Cell. 2016

98. Pore D, Parameswaran N, Matsui K, Stone MB, Saotome I, McClatchey AI, Veatch SL, Gupta N. Ezrin Tunes the Magnitude of Humoral Immunity. J Immunol Baltim Md 1950. 2013; 191(8)

99. Stone MB, Veatch SL. Steady-State Cross-Correlations for Live Two-Colour Super-Resolution Localization Data Sets. Nat Commun. 2015; 6

100. Andrews NL, Lidke KA, Pfeiffer JR, Burns AR, Wilson BS, Oliver JM, Lidke DS. Actin Restricts FcεRI Diffusion and Facilitates Antigen-Induced Receptor Immobilization. Nat Cell Biol. 2008; 10(8):955–963. [PubMed: 18641640]

101. Feder TJ, Brust-Mascher I, Slattery JP, Baird B, Webb WW. Constrained Diffusion or Immobile Fraction on Cell Surfaces: A New Interpretation. Biophys J. 1996; 70(6):2767–2773. [PubMed: 8744314]

102. Larson DR, Gosse JA, Holowka DA, Baird BA, Webb WW. Temporally Resolved Interactions between Antigen-Stimulated IgE Receptors and Lyn Kinase on Living Cells. J Cell Biol. 2005; 171(3):527–536. [PubMed: 16275755]

103. Schwartz SL, Yan Q, Telmer CA, Lidke KA, Bruchez MP, Lidke DS. Fluorogen-Activating Proteins Provide Tunable Labeling Densities for Tracking FcεRI Independent of IgE. ACS Chem Biol. 2015; 10(2):539–546. [PubMed: 25343439]

104. Shelby SA, Holowka D, Baird B, Veatch SL. Distinct Stages of Stimulated FcεRI Receptor Clustering and Immobilization Are Identified through Superresolution Imaging. Biophys J. 2013; 105(10):2343–2354. [PubMed: 24268146]

105. Szent-Gyorgyi C, Schmidt BF, Schmidt BA, Creeger Y, Fisher GW, Zakel KL, Adler S, Fitzpatrick JAJ, Woolford CA, Yan Q, et al. Fluorogen-Activating Single-Chain Antibodies for Imaging Cell Surface Proteins. Nat Biotechnol. 2008; 26(2):235–240. [PubMed: 18157118]

106. Shelby SA, Veatch SL, Holowka DA, Baird BA. Functional Nanoscale Coupling of Lyn Kinase with IgE-FcεRI Is Restricted by the Actin Cytoskeleton in Early Antigen-Stimulated Signaling. Mol Biol Cell. 2016 mbc.E16-06-0425.

107. Irving AT, Mimuro H, Kufer TA, Lo C, Wheeler R, Turner LJ, Thomas BJ, Malosse C, Gantier MP, Casillas LN, et al. The Immune Receptor NOD1 and Kinase RIP2 Interact with Bacterial Peptidoglycan on Early Endosomes to Promote Autophagy and Inflammatory Signaling. Cell Host Microbe. 2014; 15(5):623–635. [PubMed: 24746552]

108. Itano MS, Steinhauer C, Schmied JJ, Forthmann C, Liu P, Neumann AK, Thompson NL, Tinnefeld P, Jacobson K. Super-Resolution Imaging of C-Type Lectin and Influenza

Hemagglutinin Nanodomains on Plasma Membranes Using Blink Microscopy. Biophys J. 2012; 102(7):1534–1542. [PubMed: 22500753]

109. Notelaers K, Rocha S, Paesen R, Swinnen N, Vangindertael J, Meier JC, Rigo JM, Ameloot M, Hofkens J. Membrane Distribution of the Glycine Receptor α3 Studied by Optical Super-Resolution Microscopy. Histochem Cell Biol. 2014; 142(1):79–90. [PubMed: 24553792]
110. Winckler P, Lartigue L, Giannone G, De Giorgi F, Ichas F, Sibarita J-B, Lounis B, Cognet L. Identification and Super-Resolution Imaging of Ligand-Activated Receptor Dimers in Live Cells. Sci Rep. 2013; 3
111. Gao J, Wang Y, Cai M, Pan Y, Xu H, Jiang J, Ji H, Wang H. Mechanistic Insights into EGFR Membrane Clustering Revealed by Super-Resolution Imaging. Nanoscale. 2015; 7(6):2511–2519. [PubMed: 25569174]
112. Brown ACN, Oddos S, Dobbie IM, Alakoskela JM, Parton RM, Eissmann P, Neil MAA, Dunsby C, French PMW, Davis I, et al. Remodelling of Cortical Actin Where Lytic Granules Dock at Natural Killer Cell Immune Synapses Revealed by Super-Resolution Microscopy. PLOS Biol. 2011; 9(9):e1001152. [PubMed: 21931537]
113. Brown ACN, Dobbie IM, Alakoskela JM, Davis I, Davis DM. Super-Resolution Imaging of Remodeled Synaptic Actin Reveals Different Synergies between NK Cell Receptors and Integrins. Blood. 2012; 120(18):3729–3740. [PubMed: 22966166]
114. Reynwar BJ, Illya G, Harmandaris VA, Müller MM, Kremer K, Deserno M. Aggregation and Vesiculation of Membrane Proteins by Curvature-Mediated Interactions. Nature. 2007; 447(7143):461–464. [PubMed: 17522680]
115. Levental I, Veatch SL. The Continuing Mystery of Lipid Rafts. J Mol Biol. 2016
116. Bridges AA, Jentzsch MS, Oakes PW, Occhipinti P, Gladfelter AS. Micron-Scale Plasma Membrane Curvature Is Recognized by the Septin Cytoskeleton. J Cell Biol. 2016 jcb. 201512029.
117. Lee IH, Kai H, Carlson LA, Groves JT, Hurley JH. Negative Membrane Curvature Catalyzes Nucleation of Endosomal Sorting Complex Required for Transport (ESCRT)-III Assembly. Proc Natl Acad Sci U S A. 2015; 112(52):15892–15897. [PubMed: 26668364]
118. Parton RG, Simons K. The Multiple Faces of Caveolae. Nat Rev Mol Cell Biol. 2007; 8(3):185–194. [PubMed: 17318224]
119. Gabor KA, Kim D, Kim CH, Hess ST. Nanoscale Imaging of Caveolin-1 Membrane Domains In Vivo. PLOS ONE. 2015; 10(2):e0117225. [PubMed: 25646724]
120. Gabor KA, Stevens CR, Pietraszewski MJ, Gould TJ, Shim J, Yoder JA, Lam SH, Gong Z, Hess ST, Kim CH. Super Resolution Microscopy Reveals That Caveolin-1 Is Required for Spatial Organization of CRFB1 and Subsequent Antiviral Signaling in Zebrafish. PLOS ONE. 2013; 8(7):e68759. [PubMed: 23874753]
121. Grover JR, Llewellyn GN, Soheilian F, Nagashima K, Veatch SL, Ono A. Roles Played by Capsid-Dependent Induction of Membrane Curvature and Gag-ESCRT Interactions in Tetherin Recruitment to HIV-1 Assembly Sites. J Virol. 2013 JVI.03526-12.
122. Shim S-H, Xia C, Zhong G, Babcock HP, Vaughan JC, Huang B, Wang X, Xu C, Bi G-Q, Zhuang X. Super-Resolution Fluorescence Imaging of Organelles in Live Cells with Photoswitchable Membrane Probes. Proc Natl Acad Sci. 2012
123. Maarouf A, Meerschaert RL, Kelly C. Revealing Nanoscale Membrane Curvature with Polarized Localization Microscopy. OSA. 2015 p NM3C.2.
124. Anantharam A, Onoa B, Edwards RH, Holz RW, Axelrod D. Localized Topological Changes of the Plasma Membrane upon Exocytosis Visualized by Polarized TIRFM. J Cell Biol. 2010; 188(3):415–428. [PubMed: 20142424]
125. Brameshuber M, Weghuber J, Ruprecht V, Gombos I, Horváth I, Vigh L, Eckerstorfer P, Kiss E, Stockinger H, Schütz GJ. Imaging of Mobile Long-Lived Nanoplatforms in the Live Cell Plasma Membrane. J Biol Chem. 2010; 285(53):41765–41771. [PubMed: 20966075]
126. Hartley JM, Chu TW, Peterson EM, Zhang R, Yang J, Harris J, Kopeček J. Super-Resolution Imaging and Quantitative Analysis of Membrane Protein/Lipid Raft Clustering Mediated by Cell-Surface Self-Assembly of Hybrid Nanoconjugates. Chembiochem Eur J Chem Biol. 2015; 16(12):1725–1729.

127. Owen DM, Rentero C, Rossy J, Magenau A, Williamson D, Rodriguez M, Gaus K. PALM Imaging and Cluster Analysis of Protein Heterogeneity at the Cell Surface. J Biophotonics. 2010; 3(7):446–454. [PubMed: 20148419]

128. Owen DM, Williamson DJ, Magenau A, Gaus K. Sub-Resolution Lipid Domains Exist in the Plasma Membrane and Regulate Protein Diffusion and Distribution. Nat Commun. 2012; 3:1256. [PubMed: 23212385]

129. Levental I, Lingwood D, Grzybek M, Coskun U, Simons K. Palmitoylation Regulates Raft Affinity for the Majority of Integral Raft Proteins. Proc Natl Acad Sci U S A. 2010; 107(51): 22050–22054. [PubMed: 21131568]

130. Sengupta P, Jovanovic-Talisman T, Skoko D, Renz M, Veatch SL, Lippincott-Schwartz J. Probing Protein Heterogeneity in the Plasma Membrane Using PALM and Pair Correlation Analysis. Nat Methods. 2011; 8(11):969–975. [PubMed: 21926998]

131. Tobin SJ, Cacao EE, Hong DWW, Terenius L, Vukojevic V, Jovanovic-Talisman T. Nanoscale Effects of Ethanol and Naltrexone on Protein Organization in the Plasma Membrane Studied by Photoactivated Localization Microscopy (PALM). PLOS ONE. 2014; 9(2):e87225. [PubMed: 24503624]

132. Milovanovic D, Honigmann A, Koike S, Göttfert F, Pähler G, Junius M, Müllar S, Diederichsen U, Janshoff A, Grubmüller H, et al. Hydrophobic Mismatch Sorts SNARE Proteins into Distinct Membrane Domains. Nat Commun. 2015; 6:5984. [PubMed: 25635869]

133. Day CA, Kenworthy AK. Tracking Microdomain Dynamics in Cell Membranes. Biochim Biophys Acta. 2009; 1788(1):245–253. [PubMed: 19041847]

134. Kusumi A, Shirai YM, Koyama-Honda I, Suzuki KGN, Fujiwara TK. Hierarchical Organization of the Plasma Membrane: Investigations by Single-Molecule Tracking vs. Fluorescence Correlation Spectroscopy. FEBS Lett. 2010; 584(9):1814–1823. [PubMed: 20178787]

135. Pralle A, Keller P, Florin EL, Simons K, Hörber JKH. Sphingolipid–Cholesterol Rafts Diffuse as Small Entities in the Plasma Membrane of Mammalian Cells. J Cell Biol. 2000; 148(5):997–1008. [PubMed: 10704449]

136. Sevcsik E, Brameshuber M, Fölser M, Weghuber J, Honigmann A, Schütz GJ. GPI-Anchored Proteins Do Not Reside in Ordered Domains in the Live Cell Plasma Membrane. Nat Commun. 2015; 6:6969. [PubMed: 25897971]

137. Honigmann A, Mueller V, Ta H, Schoenle A, Sezgin E, Hell SW, Eggeling C. Scanning STED-FCS Reveals Spatiotemporal Heterogeneity of Lipid Interaction in the Plasma Membrane of Living Cells. Nat Commun. 2014; 5:5412. [PubMed: 25410140]

138. Machta BB, Papanikolaou S, Sethna JP, Veatch SL. Minimal Model of Plasma Membrane Heterogeneity Requires Coupling Cortical Actin to Criticality. Biophys J. 2011; 100(7):1668–1677. [PubMed: 21463580]

139. Honigmann A, Sadeghi S, Keller J, Hell SW, Eggeling C, Vink R. A Lipid Bound Actin Meshwork Organizes Liquid Phase Separation in Model Membranes. eLife. 2014; 3:e01671. [PubMed: 24642407]

140. Wang YH, Slochower DR, Janmey PA. Counterion-Mediated Cluster Formation by Polyphosphoinositides. Chem Phys Lipids. 2014; 182:38–51. [PubMed: 24440472]

141. van den Bogaart G, Meyenberg K, Risselada HJ, Amin H, Willig KI, Hubrich BE, Dier M, Hell SW, Grubmüller H, Diederichsen U, et al. Membrane Protein Sequestering by Ionic Protein-Lipid Interactions. Nature. 2011; 479(7374):552–555. [PubMed: 22020284]

142. Murray DH, Tamm LK. Clustering of Syntaxin-1A in Model Membranes Is Modulated by Phosphatidylinositol 4,5-Bisphosphate and Cholesterol. Biochemistry (Mosc). 2009; 48(21): 4617–4625.

143. Wang J, Richards DA. Segregation of PIP2 and PIP3 into Distinct Nanoscale Regions within the Plasma Membrane. Biol Open. 2012; 1(9):857–862. [PubMed: 23213479]

144. Ji C, Zhang Y, Xu P, Xu T, Lou X. Nanoscale Landscape of Phosphoinositides Revealed by Specific Pleckstrin Homology (PH) Domains Using Single-Molecule Superresolution Imaging in the Plasma Membrane. J Biol Chem. 2015; 290(45):26978–26993. [PubMed: 26396197]

145. Xu K, Babcock HP, Zhuang X. Dual-Objective STORM Reveals Three-Dimensional Filament Organization in the Actin Cytoskeleton. Nat Methods. 2012; 9(2):185–188. [PubMed: 22231642]

146. Andrade DM, Clausen MP, Keller J, Mueller V, Wu C, Bear JE, Hell SW, Lagerholm BC, Eggeling C. Cortical Actin Networks Induce Spatio-Temporal Confinement of Phospholipids in the Plasma Membrane – a Minimally Invasive Investigation by STED-FCS. Sci Rep. 2015; 5:11454. [PubMed: 26118385]

147. Mönkemöller V, Øie C, Hübner W, Huser T, McCourt P. Multimodal Super-Resolution Optical Microscopy Visualizes the Close Connection between Membrane and the Cytoskeleton in Liver Sinusoidal Endothelial Cell Fenestrations. Sci Rep. 2015; 5:16279. [PubMed: 26549018]

148. Xu K, Zhong G, Zhuang X. Actin, Spectrin and Associated Proteins Form a Periodic Cytoskeletal Structure in Axons. Science. 2013; 339(6118)

149. D'Este E, Kamin D, Göttfert F, El-Hady A, Hell SW. STED Nanoscopy Reveals the Ubiquity of Subcortical Cytoskeleton Periodicity in Living Neurons. Cell Rep. 2015; 10(8):1246–1251. [PubMed: 25732815]

150. Steshenko O, Andrade DM, Honigmann A, Mueller V, Schneider F, Sezgin E, Hell SW, Simons M, Eggeling C. Reorganization of Lipid Diffusion by Myelin Basic Protein as Revealed by STED Nanoscopy. Biophys J. 2016; 110(11):2441–2450. [PubMed: 27276262]

151. Gudheti MV, Curthoys NM, Gould TJ, Kim D, Gunewardene MS, Gabor KA, Gosse JA, Kim CH, Zimmerberg J, Hess ST. Actin Mediates the Nanoscale Membrane Organization of the Clustered Membrane Protein Influenza Hemagglutinin. Biophys J. 2013; 104(10):2182–2192. [PubMed: 23708358]

152. Burnette DT, Shao L, Ott C, Pasapera AM, Fischer RS, Baird MA, Loughian CD, Delanoe-Ayari H, Paszek MJ, Davidson MW, et al. A Contractile and Counterbalancing Adhesion System Controls the 3D Shape of Crawling Cells. J Cell Biol. 2014; 205(1):83–96. [PubMed: 24711500]

153. Kanchanawong P, Shtengel G, Pasapera AM, Ramko EB, Davidson MW, Hess HF, Waterman CM. Nanoscale Architecture of Integrin-Based Cell Adhesions. Nature. 2010; 468(7323):580–584. [PubMed: 21107430]

154. Colin-York H, Shrestha D, Felce JH, Waithe D, Moeendarbary E, Davis SJ, Eggeling C, Fritzsche M. Super-Resolved Traction Force Microscopy (STFM). Nano Lett. 2016; 16(4):2633–2638. [PubMed: 26923775]

155. Metzger H. Transmembrane Signaling: The Joy of Aggregation. J Immunol. 1992; 149(5):1477–1487. [PubMed: 1324276]

156. Coffman VC, Wu JQ. Counting Protein Molecules Using Quantitative Fluorescence Microscopy. Trends Biochem Sci. 2012; 37(11):499–506. [PubMed: 22948030]

157. Digman MA, Dalal R, Horwitz AF, Gratton E. Mapping the Number of Molecules and Brightness in the Laser Scanning Microscope. Biophys J. 2008; 94(6):2320–2332. [PubMed: 18096627]

158. Digman MA, Wiseman PW, Choi C, Horwitz AR, Gratton E. Stoichiometry of Molecular Complexes at Adhesions in Living Cells. Proc Natl Acad Sci. 2009; 106(7):2170–2175. [PubMed: 19168634]

159. Fricke F, Beaudouin J, Eils R, Heilemann M. One, Two or Three? Probing the Stoichiometry of Membrane Proteins by Single-Molecule Localization Microscopy. Sci Rep. 2015; 5:14072. [PubMed: 26358640]

160. Leake MC, Chandler JH, Wadhams GH, Bai F, Berry RM, Armitage JP. Stoichiometry and Turnover in Single, Functioning Membrane Protein Complexes. Nature. 2006; 443(7109):355–358. [PubMed: 16971952]

161. Shivanandan A, Deschout H, Scarselli M, Radenovic A. Challenges in Quantitative Single Molecule Localization Microscopy. FEBS Lett. 2014; 588(19):3595–3602. [PubMed: 24928440]

162. McEvoy AL, Hoi H, Bates M, Platonova E, Cranfill PJ, Baird MA, Davidson MW, Ewers H, Liphardt J, Campbell RE. mMaple: A Photoconvertible Fluorescent Protein for Use in Multiple Imaging Modalities. PLOS ONE. 2012; 7(12):e51314. [PubMed: 23240015]

163. Nagai T, Ibata K, Park ES, Kubota M, Mikoshiba K, Miyawaki A. A Variant of Yellow Fluorescent Protein with Fast and Efficient Maturation for Cell-Biological Applications. Nat Biotechnol. 2002; 20(1):87–90. [PubMed: 11753368]

164. Shaner NC, Campbell RE, Steinbach PA, Giepmans BNG, Palmer AE, Tsien RY. Improved Monomeric Red, Orange and Yellow Fluorescent Proteins Derived from Discosoma Sp. Red Fluorescent Protein. Nat Biotechnol. 2004; 22(12):1567–1572. [PubMed: 15558047]

165. Tsien RY. The Green Fluorescent Protein. Annu Rev Biochem. 1998; 67(1):509–544. [PubMed: 9759496]
166. Wang S, Moffitt JR, Dempsey GT, Xie XS, Zhuang X. Characterization and Development of Photoactivatable Fluorescent Proteins for Single-Molecule–based Superresolution Imaging. Proc Natl Acad Sci U S A. 2014; 111(23):8452–8457. [PubMed: 24912163]
167. Vaughan JC, Jia S, Zhuang X. Ultrabright Photoactivatable Fluorophores Created by Reductive Caging. Nat Methods. 2012; 9(12):1181–1184. [PubMed: 23103881]
168. Bhattacharjee U, Beck C, Winter A, Wells C, Petrich JW. Tryptophan and ATTO 590: Mutual Fluorescence Quenching and Exciplex Formation. J Phys Chem B. 2014; 118(29):8471–8477. [PubMed: 24927396]
169. Gruber HJ, Hahn CD, Kada G, Riener CK, Harms GS, Ahrer W, Dax TG, Knaus HG. Anomalous Fluorescence Enhancement of Cy3 and cy3.5 versus Anomalous Fluorescence Loss of Cy5 and Cy7 upon Covalent Linking to IgG and Noncovalent Binding to Avidin. Bioconjug Chem. 2000; 11(5):696–704. [PubMed: 10995214]
170. Marmé N, Knemeyer JP, Sauer M, Wolfrum J. Inter- and Intramolecular Fluorescence Quenching of Organic Dyes by Tryptophan. Bioconjug Chem. 2003; 14(6):1133–1139. [PubMed: 14624626]
171. Sauer M. Localization Microscopy Coming of Age: From Concepts to Biological Impact. J Cell Sci. 2013; 126(16):3505–3513. [PubMed: 23950110]
172. Ester M, Kriegel HP, Sander J, Xu X. A Density-Based Algorithm for Discovering Clusters in Large Spatial Databases with Noise. KDD-96 Proc. 1996; 34:226–231.
173. Andronov L, Orlov I, Lutz Y, Vonesch JL, Klaholz BP. ClusterViSu, a Method for Clustering of Protein Complexes by Voronoi Tessellation in Super-Resolution Microscopy. Sci Rep. 2016; 6:24084. [PubMed: 27068792]
174. Bar-On D, Wolter S, van de Linde S, Heilemann M, Nudelman G, Nachliel E, Gutman M, Sauer M, Ashery U. Super-Resolution Imaging Reveals the Internal Architecture of Nano-Sized Syntaxin Clusters. J Biol Chem. 2012; 287(32):27158–27167. [PubMed: 22700970]
175. Hummer G, Fricke F, Heilemann M. Model-Independent Counting of Molecules in Single-Molecule Localization Microscopy. Mol Biol Cell. 2016 mbc.E16-07-0525.
176. Rollins GC, Shin JY, Bustamante C, Pressé S. Stochastic Approach to the Molecular Counting Problem in Superresolution Microscopy. Proc Natl Acad Sci. 2015; 112(2):E110–E118. [PubMed: 25535361]
177. Coltharp C, Kessler RP, Xiao J. Accurate Construction of Photoactivated Localization Microscopy (PALM) Images for Quantitative Measurements. PloS One. 2012; 7(12):e51725. [PubMed: 23251611]
178. Lee SH, Shin JY, Lee A, Bustamante C. Counting Single Photoactivatable Fluorescent Molecules by Photoactivated Localization Microscopy (PALM). Proc Natl Acad Sci. 2012; 109(43):17436–17441. [PubMed: 23045631]
179. Veatch SL, Machta BB, Shelby SA, Chiang EN, Holowka DA, Baird BA. Correlation Functions Quantify Super-Resolution Images and Estimate Apparent Clustering due to over-Counting. PloS One. 2012; 7(2):e31457. [PubMed: 22384026]
180. Nieuwenhuizen RPJ, Lidke KA, Bates M, Puig DL, Grünwald D, Stallinga S, Rieger B. Measuring Image Resolution in Optical Nanoscopy. Nat Methods. 2013; 10(6):557–562. [PubMed: 23624665]
181. Endesfelder U, Finan K, Holden SJ, Cook PR, Kapanidis AN, Heilemann M. Multiscale Spatial Organization of RNA Polymerase in Escherichia Coli. Biophys J. 2013; 105(1):172–181. [PubMed: 23823236]
182. Bordovsky SS, Wong CS, Bachand GD, Stachowiak JC, Sasaki DY. Engineering Lipid Structure for Recognition of the Liquid Ordered Membrane Phase. Langmuir ACS J Surf Colloids. 2016
183. Alecio MR, Golan DE, Veatch WR, Rando RR. Use of a Fluorescent Cholesterol Derivative to Measure Lateral Mobility of Cholesterol in Membranes. Proc Natl Acad Sci U S A. 1982; 79(17):5171–5174. [PubMed: 6957857]
184. Honigmann A, Mueller V, Hell SW, Eggeling C. STED Microscopy Detects and Quantifies Liquid Phase Separation in Lipid Membranes Using a New Far-Red Emitting Fluorescent Phosphoglycerolipid Analogue. Faraday Discuss. 2013; 161:77-89-150. [PubMed: 23805739]

185. McLaughlin S, Wang J, Gambhir A, Murray D. PIP(2) and Proteins: Interactions, Organization, and Information Flow. Annu Rev Biophys Biomol Struct. 2002; 31:151–175. [PubMed: 11988466]

186. Oldham KB. A Gouy–Chapman–Stern Model of the Double Layer at a (Metal)/(ionic Liquid) Interface. J Electroanal Chem. 2008; 613(2):131–138.

187. Wang YH, Collins A, Guo L, Smith-Dupont KB, Gai F, Svitkina T, Janmey PA. Divalent Cation-Induced Cluster Formation by Polyphosphoinositides in Model Membranes. J Am Chem Soc. 2012; 134(7):3387–3395. [PubMed: 22280226]

188. Seo JB, Jung SR, Huang W, Zhang Q, Koh DS. Charge Shielding of PIP 2 by Cations Regulates Enzyme Activity of Phospholipase C. PLOS ONE. 2015; 10(12):e0144432. [PubMed: 26658739]

189. Merritt EA, Sarfaty S, van den Akker F, L'Hoir C, Martial JA, Hol WG. Crystal Structure of Cholera Toxin B-Pentamer Bound to Receptor GM1 Pentasaccharide. Protein Sci Publ Protein Soc. 1994; 3(2):166–175.

190. Hammond AT, Heberle FA, Baumgart T, Holowka D, Baird B, Feigenson GW. Crosslinking a Lipid Raft Component Triggers Liquid Ordered-Liquid Disordered Phase Separation in Model Plasma Membranes. Proc Natl Acad Sci U S A. 2005; 102(18):6320–6325. [PubMed: 15851688]

191. Raghunathan K, Wong TH, Chinnapen DJ, Lencer WI, Jobling MG, Kenworthy AK. Glycolipid Crosslinking Is Required for Cholera Toxin to Partition Into and Stabilize Ordered Domains. Biophys J. 2016; 111(12):2547–2550. [PubMed: 27914621]

192. Cheng PC, Dykstra ML, Mitchell RN, Pierce SK. A Role for Lipid Rafts in B Cell Antigen Receptor Signaling and Antigen Targeting. J Exp Med. 1999; 190(11):1549–1560. [PubMed: 10587346]

193. Francis ML, Ryan J, Jobling MG, Holmes RK, Moss J, Mond JJ. Cyclic AMP-Independent Effects of Cholera Toxin on B Cell Activation. II. Binding of Ganglioside GM1 Induces B Cell Activation. J Immunol. 1992; 148(7):1999–2005. [PubMed: 1312102]

194. Harder T, Simons K. Clusters of Glycolipid and Glycosylphosphatidylinositol-Anchored Proteins in Lymphoid Cells: Accumulation of Actin Regulated by Local Tyrosine Phosphorylation. Eur J Immunol. 1999; 29(2):556–562. [PubMed: 10064071]

195. Maxfield FR, Wüstner D. Analysis of Cholesterol Trafficking with Fluorescent Probes. Methods Cell Biol. 2012; 108:367–393. [PubMed: 22325611]

196. Várnai P, Balla T. Visualization of Phosphoinositides That Bind Pleckstrin Homology Domains: Calcium- and Agonist-Induced Dynamic Changes and Relationship to Myo-[3H]inositol-Labeled Phosphoinositide Pools. J Cell Biol. 1998; 143(2):501–510. [PubMed: 9786958]

197. Ratz M, Testa I, Hell SW, Jakobs S. CRISPR/Cas9-Mediated Endogenous Protein Tagging for RESOLFT Super-Resolution Microscopy of Living Human Cells. Sci Rep. 2015; 5:9592. [PubMed: 25892259]

198. Endesfelder U, Malkusch S, Flottmann B, Mondry J, Liguzinski P, Verveer PJ, Heilemann M. Chemically Induced Photoswitching of Fluorescent Probes—A General Concept for Super-Resolution Microscopy. Molecules. 2011; 16(4):3106–3118. [PubMed: 21490558]

199. Zhang M, Chang H, Zhang Y, Yu J, Wu L, Ji W, Chen J, Liu B, Lu J, Liu Y, et al. Rational Design of True Monomeric and Bright Photoactivatable Fluorescent Proteins. Nat Methods. 2012; 9(7): 727–729. [PubMed: 22581370]

200. Axelrod D, Wang MD. Reduction-of-Dimensionality Kinetics at Reaction-Limited Cell Surface Receptors. Biophys J. 1994; 66(3 Pt 1):588–600. [PubMed: 8011892]

201. McCloskey MA, Poo MM. Rates of Membrane-Associated Reactions: Reduction of Dimensionality Revisited. J Cell Biol. 1986; 102(1):88–96. [PubMed: 3001105]

202. Tanaka KAK, Suzuki KGN, Shirai YM, Shibutani ST, Miyahara MSH, Tsuboi H, Yahara M, Yoshimura A, Mayor S, Fujiwara TK, et al. Membrane Molecules Mobile Even after Chemical Fixation. Nat Methods. 2010; 7(11):865–866. [PubMed: 20881966]

203. Heerklotz H. Triton Promotes Domain Formation in Lipid Raft Mixtures. Biophys J. 2002; 83(5): 2693–2701. [PubMed: 12414701]

204. Heerklotz H, Szadkowska H, Anderson T, Seelig J. The Sensitivity of Lipid Domains to Small Perturbations Demonstrated by the Effect of Triton. J Mol Biol. 2003; 329(4):793–799. [PubMed: 12787678]

205. Fox CH, Johnson FB, Whiting J, Roller PP. Formaldehyde Fixation. J Histochem Cytochem Off J Histochem Soc. 1985; 33(8):845–853.

206. Lillemeier BF, Pfeiffer JR, Surviladze Z, Wilson BS, Davis MM. Plasma Membrane-Associated Proteins Are Clustered into Islands Attached to the Cytoskeleton. Proc Natl Acad Sci U S A. 2006; 103(50):18992–18997. [PubMed: 17146050]

207. Sochacki KA, Shtengel G, van Engelenburg SB, Hess HF, Taraska JW. Correlative Super-Resolution Fluorescence and Metal-Replica Transmission Electron Microscopy. Nat Methods. 2014; 11(3):305–308. [PubMed: 24464288]

208. Stanly TA, Fritzsche M, Banerji S, García E, de la Serna JB, Jackson DG, Eggeling C. Critical Importance of Appropriate Fixation Conditions for Faithful Imaging of Receptor Microclusters. Biol Open. 2016; 5(9):1343–1350. [PubMed: 27464671]

209. Diez S, Gerisch G, Anderson K, Müller-Taubenberger A, Bretschneider T. Subsecond Reorganization of the Actin Network in Cell Motility and Chemotaxis. Proc Natl Acad Sci U S A. 2005; 102(21):7601–7606. [PubMed: 15894626]

210. Moneron G, Medda R, Hein B, Giske A, Westphal V, Hell SW. Fast STED Microscopy with Continuous Wave Fiber Lasers. Opt Express. 2010; 18(2):1302–1309. [PubMed: 20173956]

211. Huang F, Hartwich TMP, Rivera-Molina FE, Lin Y, Duim WC, Long JJ, Uchil PD, Myers JR, Baird MA, Mothes W, et al. Video-Rate Nanoscopy Using sCMOS Camera-Specific Single-Molecule Localization Algorithms. Nat Methods. 2013; 10(7):653–658. [PubMed: 23708387]

212. Edwald E, Stone MB, Gray EM, Wu J, Veatch SL. Oxygen Depletion Speeds and Simplifies Diffusion in HeLa Cells. Biophys J. 2014; 107(8):1873–1884. [PubMed: 25418168]

213. Grotjohann T, Testa I, Reuss M, Brakemann T, Eggeling C, Hell SW, Jakobs S. rsEGFP2 Enables Fast RESOLFT Nanoscopy of Living Cells. eLife. 2012; 1:e00248. [PubMed: 23330067]

214. Guo SM, Bag N, Mishra A, Wohland T, Bathe M. Bayesian Total Internal Reflection Fluorescence Correlation Spectroscopy Reveals hIAPP-Induced Plasma Membrane Domain Organization in Live Cells. Biophys J. 2014; 106(1):190–200. [PubMed: 24411251]

215. Di Rienzo C, Gratton E, Beltram F, Cardarelli F. Fast Spatiotemporal Correlation Spectroscopy to Determine Protein Lateral Diffusion Laws in Live Cell Membranes. Proc Natl Acad Sci U S A. 2013; 110(30):12307–12312. [PubMed: 23836651]

216. Linder S, Kopp P. Podosomes at a Glance. J Cell Sci. 2005; 118(10):2079–2082. [PubMed: 15890982]

217. Greicius G, Westerberg L, Davey EJ, Buentke E, Scheynius A, Thyberg J, Severinson E. Microvilli Structures on B Lymphocytes: Inducible Functional Domains? Int Immunol. 2004; 16(2):353–364. [PubMed: 14734621]

218. Majstoravich S, Zhang J, Nicholson-Dykstra S, Linder S, Friedrich W, Siminovitch KA, Higgs HN. Lymphocyte Microvilli Are Dynamic, Actin-Dependent Structures That Do Not Require Wiskott-Aldrich Syndrome Protein (WASp) for Their Morphology. Blood. 2004; 104(5):1396–1403. [PubMed: 15130947]

219. Svitkina TM, Bulanova EA, Chaga OY, Vignjevic DM, Kojima S, Vasiliev JM, Borisy GG. Mechanism of Filopodia Initiation by Reorganization of a Dendritic Network. J Cell Biol. 2003; 160(3):409–421. [PubMed: 12566431]

220. Shtengel G, Galbraith JA, Galbraith CG, Lippincott-Schwartz J, Gillette JM, Manley S, Sougrat R, Waterman CM, Kanchanawong P, Davidson MW, et al. Interferometric Fluorescent Super-Resolution Microscopy Resolves 3D Cellular Ultrastructure. Proc Natl Acad Sci. 2009; 106(9):3125–3130. [PubMed: 19202073]

221. Hein B, Willig KI, Hell SW. Stimulated Emission Depletion (STED) Nanoscopy of a Fluorescent Protein-Labeled Organelle inside a Living Cell. Proc Natl Acad Sci. 2008; 105(38):14271–14276. [PubMed: 18796604]

222. Fu Y, Winter PW, Rojas R, Wang V, McAuliffe M, Patterson GH. Axial Superresolution via Multiangle TIRF Microscopy with Sequential Imaging and Photobleaching. Proc Natl Acad Sci. 2016; 113(16):4368–4373. [PubMed: 27044072]

223. Parmryd I, Önfelt B. Consequences of Membrane Topography. FEBS J. 2013; 280(12):2775–2784. [PubMed: 23438106]

224. Gan W, Roux B. Binding Specificity of SH2 Domains: Insight from Free Energy Simulations. Proteins. 2009; 74(4):996–1007. [PubMed: 18767163]

225. Sandermann H Jr. High Free Energy of Lipid/protein Interaction in Biological Membranes. FEBS Lett. 2002; 514(2–3):340–342. [PubMed: 11943177]

226. Stone MB, Veatch SL. Far-Red Organic Fluorophores Contain a Fluorescent Impurity. ChemPhysChem. 2014; 15(11):2240–2246. [PubMed: 24782148]

227. Sezgin E, Chwastek G, Aydogan G, Levental I, Simons K, Schwille P. Photoconversion of Bodipy-Labeled Lipid Analogues. ChemBioChem. 2013; 14(6):695–698. [PubMed: 23512865]

228. Thompson RE, Larson DR, Webb WW. Precise Nanometer Localization Analysis for Individual Fluorescent Probes. Biophys J. 2002; 82(5):2775–2783. [PubMed: 11964263]

229. Elmokadem A, Yu J. Optimal Drift Correction for Superresolution Localization Microscopy with Bayesian Inference. Biophys J. 2015; 109(9):1772–1780. [PubMed: 26536254]

230. Backlund MP, Arbabi A, Petrov PN, Arbabi E, Saurabh S, Faraon A, Moerner WE. Removing Orientation-Induced Localization Biases in Single-Molecule Microscopy Using a Broadband Metasurface Mask. Nat Photonics. 2016; 10(7):459–462. [PubMed: 27574529]

231. Ries J, Kaplan C, Platonova E, Eghlidi H, Ewers H. A Simple, Versatile Method for GFP-Based Super-Resolution Microscopy via Nanobodies. Nat Methods. 2012; 9(6):582–584. [PubMed: 22543348]

232. Churchman LS, Ökten Z, Rock RS, Dawson JF, Spudich JA. Single Molecule High-Resolution Colocalization of Cy3 and Cy5 Attached to Macromolecules Measures Intramolecular Distances through Time. Proc Natl Acad Sci U S A. 2005; 102(5):1419–1423. [PubMed: 15668396]

233. Grimm JB, English BP, Chen J, Slaughter JP, Zhang Z, Revyakin A, Patel R, Macklin JJ, Normanno D, Singer RH, et al. A General Method to Improve Fluorophores for Live-Cell and Single-Molecule Microscopy. Nat Methods. 2015; 12(3):244–250. [PubMed: 25599551]

234. Chozinski TJ, Gagnon LA, Vaughan JC. Twinkle, Twinkle Little Star: Photoswitchable Fluorophores for Super-Resolution Imaging. FEBS Lett. 2014; 588(19):3603–3612. [PubMed: 25010263]

235. Lavis LD, Grimm JB, English BP, Muthusamy AK, Mehl BP, Dong P, Brown TA, Liu Z, Lionnet T. Bright Photoactivatable Fluorophores for Single-Molecule Imaging. bioRxiv. 2016:66779.

236. Li D, Shao L, Chen B-C, Zhang X, Zhang M, Moses B, Milkie DE, Beach JR, Hammer JA, Pasham M, et al. Extended-Resolution Structured Illumination Imaging of Endocytic and Cytoskeletal Dynamics. Science. 2015; 349(6251):aab3500. [PubMed: 26315442]

237. Zanacchi FC, Lavagnino Z, Faretta M, Furia L, Diaspro A. Light-Sheet Confined Super-Resolution Using Two-Photon Photoactivation. PLOS ONE. 2013; 8(7):e67667. [PubMed: 23844052]

238. Urban BE, Yi J, Chen S, Dong B, Zhu Y, DeVries SH, Backman V, Zhang HF. Super-Resolution Two-Photon Microscopy via Scanning Patterned Illumination. Phys Rev E. 2015; 91(4):42703.

239. McGorty R, Schnitzbauer J, Zhang W, Huang B. Correction of Depth-Dependent Aberrations in 3D Single Molecule Localization and Super-Resolution Microscopy. Opt Lett. 2014; 39(2):275–278. [PubMed: 24562125]

240. Liu S, Kromann EB, Krueger WD, Bewersdorf J, Lidke KA. Three Dimensional Single Molecule Localization Using a Phase Retrieved Pupilfunction. Opt Express. 2013; 21(24):29462–29487. [PubMed: 24514501]

241. Hanser BM, Gustafsson MGL, Agard DA, Sedat JW. Phase Retrieval for High-Numerical-Aperture Optical Systems. Opt Lett. 2003; 28(10):801–803. [PubMed: 12779151]

242. Shechtman Y, Weiss LE, Backer AS, Sahl SJ, Moerner WE. Precise Three-Dimensional Scan-Free Multiple-Particle Tracking over Large Axial Ranges with Tetrapod Point Spread Functions. Nano Lett. 2015; 15(6):4194–4199. [PubMed: 25939423]

243. Quirin S, Pavani SRP, Piestun R. Optimal 3D Single-Molecule Localization for Superresolution Microscopy with Aberrations and Engineered Point Spread Functions. Proc Natl Acad Sci. 2012; 109(3):675–679. [PubMed: 22210112]

244. Shtengel G, Wang Y, Zhang Z, Goh WI, Hess HF, Kanchanawong P. Imaging Cellular Ultrastructure by PALM, iPALM, and Correlative iPALM-EM. Methods Cell Biol. 2014; 123:273–294. [PubMed: 24974033]

Biographies

Matthew Stone

Matthew Stone received his B.S. in Physics in 2010 from Clemson University and recently completed his Ph.D. in Biophysics in 2016 at the University of Michigan under the supervision of Sarah Veatch. His thesis work focuses on observing the nanoscale organization of cell plasma membrane lipids and receptors, focusing on the B cell receptor.

Sarah Shelby

Sarah Shelby received her B.S. in Chemical Biology in 2008 from UC Berkeley and her Ph.D. in Biophysics in 2015 from Cornell University under the supervision of Professors Barbara Baird, David Holowka, and Warren Zipfel. Her thesis work focused on characterization of the organization, dynamics, and early signaling interactions of the IgE receptor, FcεRI, in mast cells using super-resolution fluorescence localization microscopy. She is currently a post-doctoral researcher in Professor Sarah Veatch's group in the Biophysics department at the University of Michigan. Her current research is directed toward super-resolution imaging of the B cell receptor in living cells.

Sarah Veatch

Sarah Veatch obtained her BS in physics from MIT and her PhD in Physics at the University of Washington. In her graduate work with Sarah Keller, she mapped phase diagrams of the then newly identified miscibility phase transition in purified lipid bilayer membranes by fluorescence microscopy and NMR. These simplified bilayer systems are thought to be a minimal analog for 'lipid rafts,' the nano-scale, lipid-mediated heterogeneity observed in cell plasma membranes. Her postdoctoral work with Barbara Baird and David Holowka at Cornell University sought to translate this work from simple model membranes into compositionally complex biological membranes by focusing on bilayers isolated from live cells, where she found evidence that cell plasma membranes have compositions biologically tuned to be close to a miscibility critical point at growth temperatures. Sarah Veatch is currently an Assistant Professor of Biophysics and Physics at the University of Michigan. One major focus of her lab is to use and develop super-resolution imaging methods to better understand how lipid mixing gives rise to biological functions in mammalian cells.

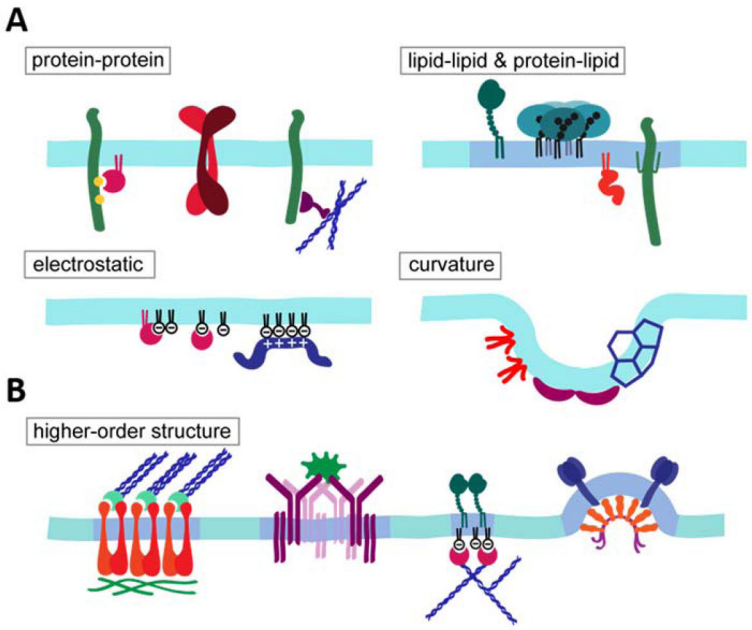

Figure 1. Fundamental interactions between membrane components are the building blocks for large-scale co-operative events

A) Fundamental interactions between membrane components include protein-protein interactions, lipid-lipid and lipid-protein interactions, electrostatic interactions, and membrane curvature-based interactions. **B)** A sample of large-scale cooperative events occurring at the membrane are shown here, including membrane adhesion, immune receptor activation, cytoskeleton corralling, and membrane vesiculation and budding. These events are comprised of many fundamental interactions between components.

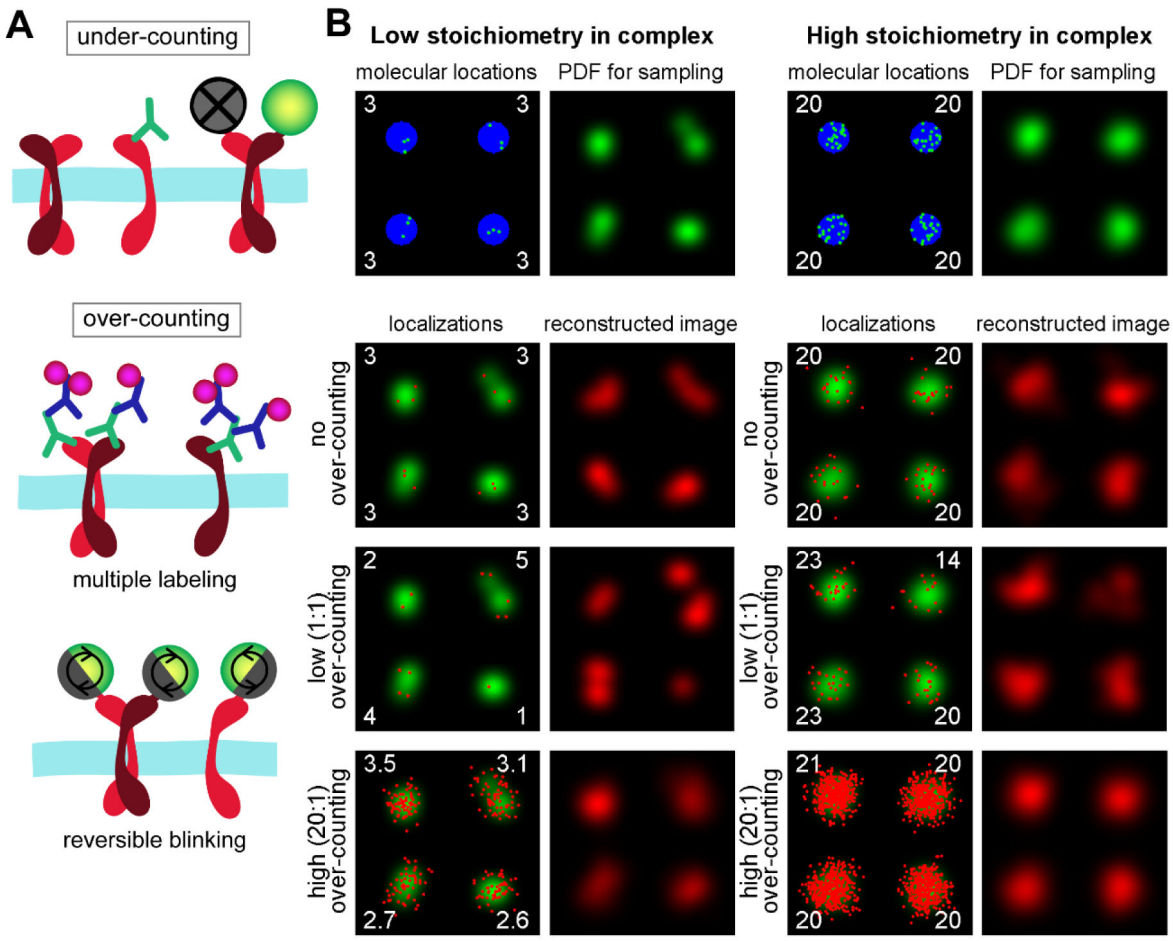

Figure 2. Over-counting in super-resolution fluorescence localization microscopy

(A) Several schematic examples of how individual labeled molecules can be under- or over-counted in a super-resolution fluorescence localization microscopy measurement. (B) Simulations of molecular counting in complexes. First, either 3 (left) or 20 (right) molecular locations were chosen at positions within each of the blue circles representing complexes with radii of 40nm. When present, the white numbers in corners represent the counts detected in each complex divided by the number of times each molecule is detected on average. Molecular positions were converted into a probability distribution function (PDF) by blurring with a Gaussian function with standard deviation equal to the localization precision (20nm). The bottom panels show this PDF stochastically sampled according to different rules alongside the reconstructed image associated with this sampling. In the case of ‘no over-counting’ the Gaussian point spread function (PSF) is sampled exactly once for each molecular position. This sampling accurately counts the stoichiometry of the complex. For the case of ‘low over-counting’, each PSF is sampled on average once, or the entire PDF is sampled either 12 (left) or 80 (right) times. Here, the counts detected per complex vary widely, with greater relative variance when the stoichiometry is low. For the case of ‘high over-counting’, each PSF is sampled on average 20 times. High over-counting reduces the variance in molecules detected per complex and produces reconstructed images that more closely resemble the original PDF.

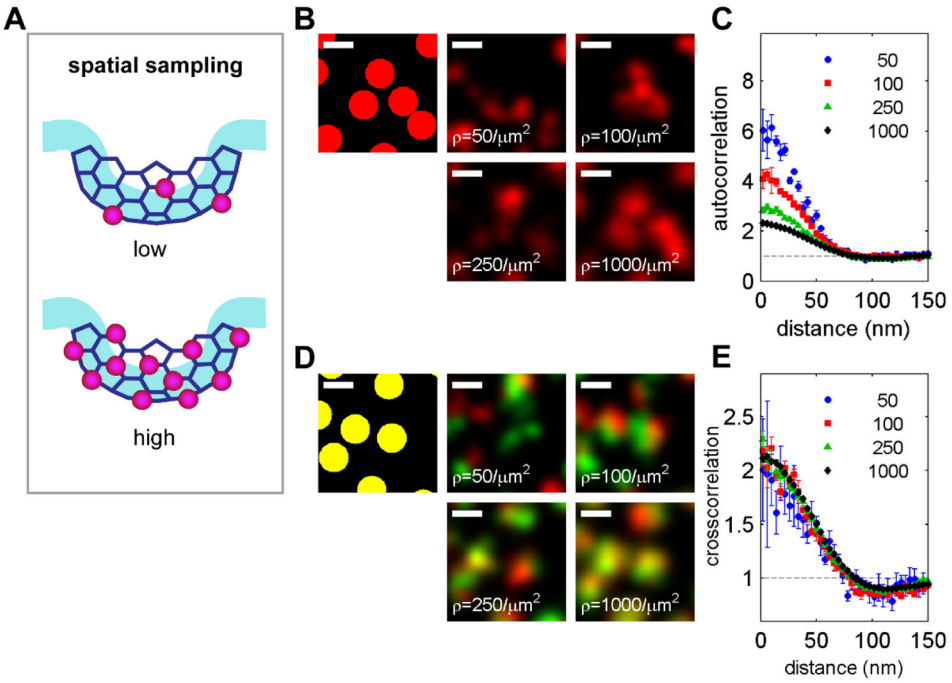

Figure 3. Spatial sampling and over-counting impact the quality and quantitation of super-resolved images

(A) A schematic representation of low and high spatial sampling of a membrane structure. (B) Increased spatial sampling greatly improves the quality and information content of reconstructed super-resolution images. The underlying structure shown at the top left is made up of randomly placed circles with radius of 50nm. This structure is randomly sampled at the surface density indicated (without replacement) to select labeled molecules. This molecular distribution is then used to generate a PDF (not shown) by blurring centers with a Gaussian shaped PSF with standard deviation of 20nm. This PDF is resampled to simulate over-counting, such that the average molecule is localized 5 times, then localizations are blurred by the same PSF to generate the reconstructed images shown. More under-sampled images appear more self-clustered because the eye is drawn to individual over-counted components rather than the underlying structure. **(C)** Autocorrelation functions for the conditions shown in A, where error-bars indicate the standard error of the mean between 5 trials. Autocorrelation functions provide a quantitative measure of self-clustering where a value of 1 indicates a random distribution, and values greater than one indicate self-clustering. Autocorrelation functions are influenced by over-counting in a spatial sampling dependent manor[142], with lower spatial sampling giving rise to more apparent self-clustering. **(D)** Images are generated in the same way as in A, but with the underlying structure sampled by two distinguishable target molecules (without replacement) at the densities indicated. Note that co-clustering is not apparent by eye at the lower sampling densities shown. **(E)** Cross-correlation functions tabulated between distinguishable probes for the examples shown in C. In contrast to autocorrelations, crosscorrelations do not depend on spatial sampling density beyond affecting signal to noise[142]. Scale-bars are 100nm.

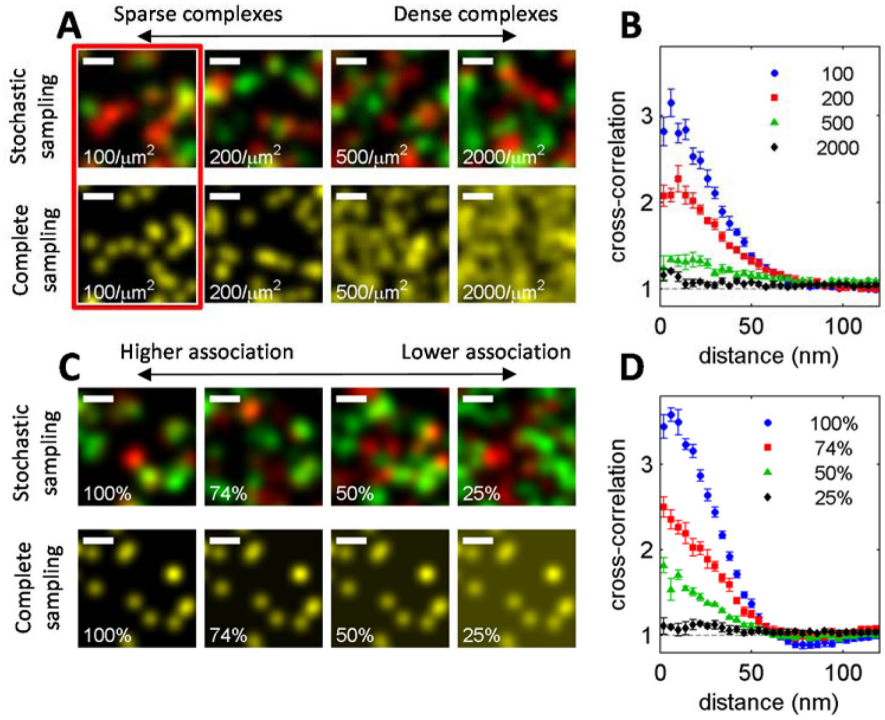

Figure 4. Measurements of co-clustering require greater sensitivity when co-clusters are distributed at high average density and when co-clustering is incomplete

(A) Reconstructed images of molecular complexes containing two distinguishable components that are constitutively associated and randomly distributed at the indicated surface density. **(B)** Cross-correlation functions from simulations like those shown in A indicate that co-clustering is more easily observed when molecular complexes are sparsely distributed at the lateral resolution probed. **(C)** Reconstructed images of molecular complexes at a density of 100/μm^2 (as indicated in A by red box) containing two distinguishable components that are partially associated, where the percentage of molecules present in complexes varies as indicated. **(D)** Cross-correlation functions from simulations like those shown in C indicate that co-clustering can be hard to detect when the fraction of labeled molecules in complexes is low. For A and C, the top image is a simulation where aggregates are both under-sampled and probes are over-counted as described in Figure 3. The bottom images represent what would be observed with perfect sampling and extensive over-counting with a 20nm localization precision. In these simulations, structures are 4nm^2 objects distributed randomly at the indicated surface density. Each point is observed on average 5 times. Scale-bars are 100nm.

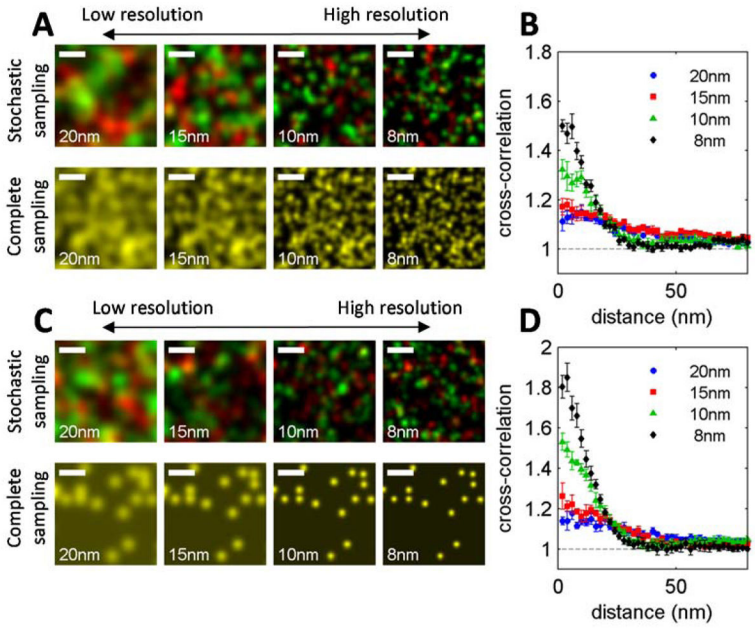

Figure 5. Improved resolution enhances sensitivity and contrast

(A) Reconstructed images of molecular complexes containing two distinguishable components present at high surface density (2000/μm^2). Simulations sample identical underlying structures generated at the localization precisions shown. **(B)** Cross-correlation functions from simulations like those shown in A have a higher amplitude at short distances with improved resolution. This occurs because complexes present at a fixed surface density become more distinguishable as the resolution improves. **(C)** Reconstructed images of molecular complexes present at a low surface density (100/μm^2) where only 25% of components reside within complexes. Simulations sample identical underlying structures are generated at the localization precisions shown. **(D)** Cross-correlation functions from simulations like those shown in C have higher amplitude at short distances with improved resolution. This occurs because the complexed proteins have higher contrast compared to the bulk as the localization precision improves. Simulations are conducted exactly as described for Figure 4 with the exception that over-counting peaks and images are blurred by a Gaussian with the specified standard deviation. Scale-bars are 100nm.